MODULATION OF MAMMALIAN SPERM MOTILITY IS CRUCIAL TO FERTILIZATION

A Dissertation

Presented to the Faculty of the Graduate School

of Cornell University

In Partial Fulfillment of the Requirements for the Degree of

Doctor of Philosophy

by

Haixin Chang

January 2012

MODULATION OF MAMMALIAN SPERM MOTILITY IS CRUCIAL TO FERTILIZATION

Haixin Chang, Ph. D.

Cornell University 2012

Hyperactivation, a motility pattern of mammalian sperm in the oviduct, is essential to fertilization. Hyperactivation helps sperm to swim effectively through oviductal mucus, to escape from the sperm reservoir, and to penetrate the cumulus matrix and zona pellucida of the oocyte. Hyperactivation is characterized by asymmetrical flagellar beating and an increase of cytoplasmic Ca^{2+}. We observed that when mouse sperm hyperactivate during capacitation in vitro, the amplitude of the flagellar bend that forms in the same orientation as the hook of the head is greatly increased. We defined this as pro-hook beating. We established that pro-hook beating is stimulated by an influx of Ca^{2+} through CATSPER channels and is associated with an increase of intracellular pH. However, an increase of flagellar bend amplitude in the opposite direction can be induced by treating sperm with thimerosal to stimulate release of Ca^{2+} from internal stores. We defined this as anti-hook beating. We also demonstrated that anti-hook beating is dominant over pro-hook beating; that is, when sperm are simultaneously or sequentially subjected to treatments that stimulate pro-hook and anti-hook beating, then the sperm will swim using the anti-hook beating pattern. Different protein phosphorylation patterns were detected in extracts of sperm

that produced these two different flagellar beat patterns, indicating the involvement of different signaling pathways. In order to better understand how sperm movement is regulated in the oviduct, we mated wild-type female mice with Acr-EGFP males, whose sperm with fluorescent acrosomes enabled us to locate sperm moving within the oviduct easily. Oviducts were removed shortly before or after ovulation to record sperm movement within. Hyperactivated sperm in the isthmic reservoir detached frequently from the epithelium and then reattached. However, most sperm found in the ampulla remained bound to epithelium throughout the observation period of several minutes. In both regions, most sperm produced anti-hook bends. Sperm were observed to detach from epithelium in both the ampulla and isthmus during strong contractions of the wall of the oviduct. These observations indicate that sperm continue to bind to oviductal epithelium after they leave the isthmic reservoir and may be assisted in detaching by muscular contractions; furthermore, the intracellar Ca^{2+} store in sperm is likely to be involved in modulating sperm movement. Together with the in vitro experiments, we conclude that sperm motility is modulated to guide the ascent of sperm up the oviduct and toward the oocytes, with different Ca^{2+} signaling pathways underlying this process.

BIOGRAPHICAL SKETCH

Haixin Chang received her Bachelor of Science degree in June 2005 from the Department of Life Science in Shanxi University, China. Since September 2005, she has been a graduate student in the field of Zoology and Wildlife Conservation, Department of Biomedical Sciences in Cornell University. She became a Ph.D. candidate in May 2008. Dr. Susan Suarez is Haixin's mentor.

ACKNOWLEDGMENTS

I would like to give my sincere thanks to my mentor Dr. Susan Suarez who guided and supported me throughout my entire Ph.D. study in Cornell University.

I would like to thank the other two members in my special committee: Drs. Alex Travis and Clare Fewtrell, for their guidance throughout my Ph.D study.

I also would like to thank the following people who were or are members of Dr. Suarez's lab for their generous support and collaboration: Dr. Osamu Kawase, Dr. George Ignotz, Dr. Pei-Hsuan (Chris) Hung, Shailly Prasad, Srivarsha Koripella, and Thomas Yaros.

I want to give special thanks to Drs. Harvey Florman and Keith Sutton in the University of Massachusetts for giving us the Acr-EGFP transgenic male mice, and Robert Munroe who provided me with many mice from his research colony.

Great appreciation to NSF and NIH for funding grants NSF MCB0421855 and NIH 1R03HD062471-01.

At the end, I would like to thank my family for their generous love and support.

TABLE OF CONTENTS

LIST OF TABLES

LIST OF FIGURES

CHAPTER 1

Re-thinking the relationship between hyperactivation and chemotaxis in mammalian sperm*

ABSTRACT

Hyperactivation, a motility pattern of mammalian sperm in the oviduct, is essential to fertilization. Hyperactivation helps sperm to swim effectively through oviductal mucus, to escape from the sperm reservoir, and to penetrate the cumulus matrix and zona pellucida of the oocyte. There is some evidence that mammalian sperm can undergo chemotaxis; however, the relationship of chemotaxis to hyperactivation is unknown. Ca^{2+} signaling is involved in hyperactivation and implicated in chemotaxis as well. *In vivo*, sperm hyperactivate in the lower oviduct, far from the cumulus-oocyte complex and possibly beyond the influence of chemotactic gradients emanating from the oocyte or cumulus. Thus, sperm are likely to be hyperactivated before sensing chemotactic gradients. Chemotactic signals might modulate hyperactivation to direct sperm toward oocytes as they reach a region of influence. Ca^{2+} -directed modulation of hyperactivation is a potential mechanism of this process.

Figure 1.4 is from Ho and Suarez (2001), reference [72].

*Chang H, Suarez SS. the Relationship Between Hyperactivation and Chemotaxis in Mammalian Sperm. Biol Reprod 2010; 83:507-513.

INTRODUCTION

In mammals, although the male deposits thousands or even millions of sperm into the female reproductive tract, this large number alone does not guarantee fertilization. Successful transport of the sperm, penetration of the egg coverings, and fusion of the sperm and egg depend on both the ability of sperm to respond to the female reproductive environment and the ability of female to affect the progress and physiological state of the sperm.

In 1970, Yanagimachi observed that hamster sperm swimming in the oviduct exhibited an extremely vigorous motility pattern with high-amplitude asymmetrical flagellar beating [1], which he later defined as hyperactivation. This first observation opened the door to a new area of research. Since then, considerable knowledge has been accumulated about this sperm motility pattern in various mammalian species.

Chemotaxis is defined in this review as the process by which sperm are guided by a chemical gradient to reach the oocyte. Chemotactic behavior and underlying molecular mechanisms have been well documented in some species of marine invertebrates with external fertilization (reviewed by Kaupp *et al.* [2]). In contrast, the existence of chemotaxis in mammalian fertilization is still a topic of debate. Although evidence for chemotaxis of mammalian sperm appeared as long ago as 1958 [3, 4], intensive research on the subject began only in the early 1990's. At that time, human sperm were reported to be chemotactically attracted by follicular fluid [5-7], which was thought to be transported into the oviduct along with the oocyte/cumulus complex.

Since then, evidence has been published for chemotaxis in other mammalian species (reviewed by Eisenbach and Giojalas [8]).

Hyperactivation and chemotaxis have been studied in mammals by different groups of investigators, and the relationship between the two phenomena is not understood. This mini-review summarizes the current knowledge of hyperactivation and chemotaxis in mammals and proposes a model for the relationship.

CONTRASTING DEFINITIONS OF HYPERACTIVATION AND CHEMOTAXIS

Hyperactivation is characterized by high-amplitude, asymmetrical flagellar beating. If hyperactivated sperm are placed on a microscope slide in aqueous medium, they swim in a circular or helical trajectory due to the asymmetrical beating. Before hyperactivation, the swimming path of sperm is relatively straight, due to low-amplitude, nearly symmetrical flagellar beating. This behavior is referred to as activated or progressive motility. Before ejaculation, mature sperm are stored in a weakly motile or immotile state in the caudal epididymis and vas deferens. They quickly activate when they are released by ejaculation or by dissection into an appropriate medium, which usually must contain bicarbonate and calcium ions [9-11].

Whereas hyperactivation is defined as a flagellar beat pattern, chemotaxis is defined as a pattern of the swimming path of sperm with reference to a chemical

gradient. These are different kinds of definitions. Thus, sperm may use hyperactivation, perhaps intermittently, to achieve chemotaxis.

Much more has been elucidated about the process of sperm chemotaxis in some marine invertebrate species and these species have served as models for the study of chemotaxis. In a variety of marine invertebrate species, including the sea urchin *Arbacia punctulata*, the response of sperm to chemotactic signals from the egg has been shown to involve a "turn and run" pattern, in which the swimming trajectory vacillates between high and low curvature, due to alternation between asymmetrical and nearly symmetrical flagellar beating. This alteration produces a loosely helical pattern with an axis that is directed toward the source of the attractant (reviewed by Kaupp *et al.* [2]) (Figure 1.1). The turn and run pattern has not been clearly seen in mammalian sperm. In fact, the details of the flagellar response of mammalian sperm to chemoattractants are not well known. The most detailed account was a figure showing human sperm responding to a gradient of bourgeonal [12]. In this figure, the flagellar beat switches from symmetrical to asymmetrical for only one beat cycle, and then returns to a symmetrical beat. The single cycle switch serves to orient the sperm into the gradient. Repeated alteration between symmetrical and asymmetrical beating, as seen in invertebrate sperm, has not been shown for mammalian sperm. It is possible that the flagellar response pattern of mammalian sperm is not well known because direct observation of swimming patterns of mammalian sperm tested with putative chemotactic agents has been limited in most studies by a very low response rate of the

sperm [13]. It is difficult to capture the flagellar beating patterns of the few sperm that actually respond.

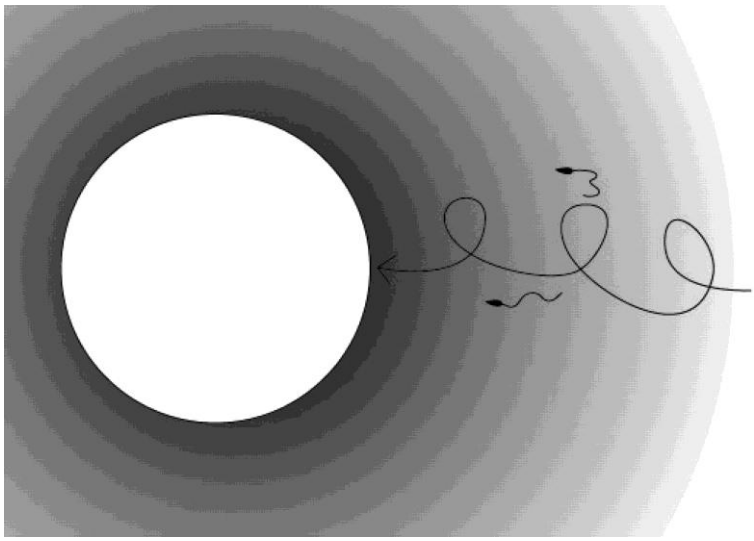

Figure 1.1. "Turn and run" model in marine sperm chemotaxis. Sperm sense changes in chemoattractant concentrations (gray) by using asymmetrical bends to “turn”. The “run” phase follows during which sperm swim up the chemoattractant gradient in a relatively straight trajectory propelled by symmetrical flagellar beating. The trajectory of repeated “turn and run” forms a helix with an axis directed toward the source of the attractant (white circle).

CONTRASTING FUNCTIONS OF HYPERACTIVATION AND CHEMOTAXIS

Hyperactivation plays various roles during the sperm’s progress toward the oocyte. First, sperm use hyperactivation to move out of the oviductal storage reservoir. Sperm are held in the reservoir by attaching to the oviductal epithelium (reviewed by Suarez and Pacey [14]) and hyperactivation assists sperm in breaking free from the attachment [15-18]. Second, hyperactivation provides sperm with a greater thrusting

force to swim through viscoelastic substances in the oviduct [19-21], which include mucus secreted by the oviductal epithelium and the matrix of the oocyte's cumulus oophorus. Lastly, hyperactivation is required by sperm to penetrate the zona pellucida of the oocyte in order to reach and fuse with the oocyte plasma membrane [22-24].

By definition, chemotaxis is the directed movement of sperm toward the source of a chemical gradient, usually considered to be an oocyte. Whereas, the functions attributed so far to hyperactivation all assist sperm in reaching the oocyte, they only do so indirectly. If we accept the definition of hyperactivation as asymmetrical flagellar beating, it is unlikely that continuous hyperactivation would lead sperm toward an oocyte, unless the flagellar beat pattern is modified intermittently, as discussed below.

SPECIFIC MOLECULAR TRIGGERS FOR CHEMOTAXIS AND HYPERACTIVATION IN MAMMALIAN SPERM REMAIN ELUSIVE

Even though hyperactivation has been studied extensively since it was first reported in 1970 [1], the physiological factor that switches on hyperactivation *in vivo* remains elusive. Hyperactivation occurs in the isthmus of the oviduct before ovulation [15, 25], so at least one trigger should be available within the preovulatory oviduct.

The discovery of CATSPER channels in sperm provided a new perspective on this issue. There are four known CATSPER genes (CATSPER 1-4), coding for

proteins structurally similar to subunits of conventional voltage-gated cation channels. Sperm from male mice that are null mutants for any of the four known CATSPER genes cannot hyperactivate, because all four are required for channel formation [26, 27]. CATSPER channels are activated by alkaline depolarization ([28], and reviewed by Navarro [29]); therefore, a change in ionic environment in the oviduct, particularly an increase in the pH of oviduct fluid, could activate the CATSPER channels and raise intracellular pH to initiate hyperactivation. In rhesus monkeys, the pH in the lumen of the oviducts was measured to be 7.1–7.3 during the pre-ovulatory phase and increased to 7.5–7.8 at ovulation [30]; however, hyperactivation may occur before this rise.

A variety of chemoattractants have been identified in various marine invertebrate species, ranging from amino acids and peptides to lipids and sulfated steroids. The species-specificity of the chemoattractants is high in some species, such as hydromedusae and certain ophiuroids, presumably to avoid interspecies fertilization (reviewed by Eisenbach [31]), but not in others, such as some echinoderms ([32], reviewed by Garbers [33] and Suzuki [34]). In mammals, some putative chemoattractants lack species-specificity [35], while others may not, as discussed below. Certainly, species-specificity is of less concern in mammals than in marine invertebrate species that broadcast their gametes into the water.

Human follicular fluid [6, 7, 36-38] or media conditioned by cumulus cells [39, 40] have been reported to attract sperm. Progesterone is considered to be the primary active agent in follicular fluid [38, 41, 42] and cumulus cells secrete progesterone [43]; therefore, a gradient of progesterone could form within and surrounding the cumulus

mass in the oviduct. Progesterone gradients have been shown to produce chemotactic behavior in human [44] and rabbit sperm [42]. Progesterone gradients in picomolar ranges or up to micromolar levels have been reported to produce chemotaxis [44-46]. Nevertheless, at least one study suggests that other factors besides progesterone present in the follicular fluid act as chemoattractants as well. In this study, chemotactic behavior of human sperm was detected in follicular fluid that had been depleted of steroids [47].

There are two problems associated with demonstrating that progesterone is a chemoattractant. The first is that only low percentages of sperm have been seen to orient into chemotactic gradients of progesterone [13, 44], requiring careful statistical analysis to demonstrate that the response is significant. The second is that concentrations from μM to mM progesterone have been shown to induce acrosome reactions in mouse and human sperm [43, 48], and there is evidence that the high levels of progesterone are also involved in priming sperm to undergo acrosome reactions stimulated by zona pellucida proteins [48-50]. When sperm undergo the acrosome reaction, the acrosomal region of the head becomes particularly sticky and could thus cause sperm to accumulate toward the source of the progesterone gradient. Nevertheless, it is plausible that low levels of progesterone in the oviduct or peripheral cumulus mass could function in chemotaxis, whereas higher levels deeper within the cumulus mass could prime or induce acrosome reactions.

There is also some evidence that odorant-like molecules function as chemoattractants to mammalian sperm. Immunolabeling studies have localized

odorant receptors to the base of flagellum or in the flagellar midpiece of mature dog [51] and rat [52] sperm. A human odorant receptor specific to the testis was identified as hOR17. A ligand for this receptor, bourgeonal, was reported to cause human sperm to swim up a gradient [12, 53]. In mouse sperm, an odorant receptor was identified with a known ligand of lyral, which is an analog of bourgeonal. In this study, sperm were seen to accumulate around the tip of a microcapillary tube which contained lyral; however, some of the accumulation was attributed to immobilization of sperm by high concentrations of lyral [54]. The proposed role of these odorants as chemoattractants has not been advanced or confirmed by other laboratories since it was reported in 2003 and 2004. Furthermore, bourgeonal and lyral are both floral products and the mammalian equivalents have not yet been identified. The lack of confirmative studies and identification of mammalian equivalents to floral odorants raises doubts about the role of odorants in mammalian sperm chemotaxis.

Ca^{2+} SIGNALING IS COMMON TO BOTH HYPERACTIVATION AND CHEMOTAXIS

Although little is known of the triggers of hyperactivation and chemotaxis in mammalian sperm, there is strong evidence that a rise in cytoplasmic Ca^{2+} is required for hyperactivation. Omission of Ca^{2+} from the medium prevents the development of hyperactivation [55, 56]. Increasing cytoplasmic Ca^{2+} by treating sperm with Ca^{2+} ionophores A23187 or ionomycin induces hyperactivation [57-59], and

hyperactivation is inhibited by Ca^{2+} channel blockers [22]. Fluorescent Ca^{2+} indicators report that Ca^{2+} levels in the flagella of hyperactivated hamster sperm are higher than those of activated sperm [60, 61]. Bull sperm demembranated by detergents and reactivated by exogenous ATP show activated motility in low levels of Ca^{2+} (~50 nM) and hyperactivated motility at higher levels (~400 nM) [62]. Altogether, these observations indicate that a rise in cytoplasmic Ca^{2+}, particularly within the cytoplasmic compartment of the flagellum, plays a crucial role in the induction of hyperactivation, presumably downstream from any signaling molecule or other trigger.

How the Ca^{2+} level rises within the flagellum to promote hyperactivation is not completely clear. The predominant source of Ca^{2+} during hyperactivation is extracellular Ca^{2+} influx through CATSPER channels (see reviews in Navarro *et al.* [29], Publicover *et al.* [63], and Suarez [64]; also see [65]). As pointed out above, sperm from male mice that are null mutants for any of the four known CATSPER genes cannot hyperactivate [26, 27]. Other Ca^{2+} channels have been detected in mammalian sperm flagella, including transient receptor potential [66], cyclic-nucleotide-gated [67], and voltage-gated Ca^{2+} channels (reviewed in Carlson *et al.* [26] and Darszon *et al.* [68]); however, it is unclear whether any of these channels play a role in hyperactivation (reviewed in Carlson *et al.* [26]). At this point, inactivation of Ca^{2+} channel genes other than CATSPER genes have not eliminated hyperactivation; however, not all possible Ca^{2+} channel genes expressed in sperm have been tested by inactivation because silencing of some has produced embryonic lethality, thus preventing investigation of the effects on sperm.

In addition to channels in the plasma membrane, Ca^{2+} can also be provided to the flagellum in mammalian sperm by the intracellular Ca^{2+} store in the redundant nuclear envelope (RNE) that is located at the base of the flagellum. Immunological labeling reveals that the RNE contains IP_3 receptors [69]. Treatment of bull sperm with either thapsigargin or thimerosal, which induce release from Ca^{2+} stores [70, 71], rapidly induces asymmetrical flagellar beating, even in the absence of available extracellular Ca^{2+} [72].

Is Ca^{2+} signaling involved in mammalian sperm chemotaxis? In marine invertebrate species, sperm respond to chemoattractants from oocytes via Ca^{2+}-regulated changes in flagellar beating asymmetry. In the sea urchin species *Arbacia punctulata*, very low concentrations of the peptide resact, which is secreted by oocytes, chemotactically attract sperm [73]. Binding of the peptide to a receptor-type guanylyl cyclase on the sperm membrane triggers a series of events leading to the opening of voltage-dependent Ca^{2+} channels, which triggers the "turn and run" response (reviewed by Kaupp *et al.* [2]). A rise in flagellar Ca^{2+} in response to a specific chemoattractant has also been recorded for sperm from the ascidian *Ciona intestinalis* [74]. The rise in Ca^{2+} is intermittent, and it is related to the turning response [74, 75]. Nevertheless, because signaling components upstream of Ca^{2+}, particularly the receptor-type guanylyl cyclase, have not been identified in mammalian sperm, the invertebrate model may not be informative in this regard.

As discussed above, there is some evidence that human and mouse sperm possess odorant receptors and exhibit chemotactic responses to gradients of specific

odorants. Human sperm exposed to the odorant bourgeonal exhibit a Ca^{2+} rise that originates in the flagellar midpiece [12, 53, 76]. In mouse sperm, the odorant lyral triggers a similar increase in Ca^{2+} [54]. Nevertheless, the Ca^{2+} response of sperm to gradients of odorant attractants is not known.

Although the role of progesterone in chemotaxis is debatable, it has been reported that human sperm exposed to gradients of progesterone exhibit a gradual increase in intracellular Ca^{2+} and about a third of the responding sperm exhibit oscillations in Ca^{2+} at the base of flagellum. The flagella of responding sperm show temporary increases in bend amplitude during Ca^{2+} peaks [45]. Nevertheless, it is not clear whether the Ca^{2+} responses to progesterone, if physiological, are involved in chemotaxis or hyperactivation, or both.

A PROPOSAL FOR THE RELATIONSHIP OF HYPERACTIVATION TO CHEMOTAXIS

In rabbits and mice, it has been observed that sperm begin to hyperactivate in the lower oviduct before ovulation [15, 25]. They do this as part of the process of releasing themselves from the sperm storage reservoir [16, 18]. Prior to release, sperm are held in the reservoir (Figure 1.2) by binding to the surface of the oviductal epithelium. There is evidence that release is brought about by a combination of shedding of oviductal binding proteins from the head of the sperm and by initiation of hyperactivation (reviewed by Suarez [77]). Because the onset of hyperactivation and

release from storage precedes ovulation, sperm are likely already hyperactivated before they become exposed to any chemoattractants that emanate from the oocyte/cumulus complex. Hyperactivation also begins in the oviduct, at least in the mouse, quite far from the site of fertilization. A long length of coiled oviduct comes between the sperm in the reservoir and the newly-ovulated oocytes (Figure 1.2). Therefore, we propose that chemoattractants modulate the flagellar beating of sperm that are already hyperactivated in order to re-direct the sperm into a chemoattractant gradient and toward the oocyte.

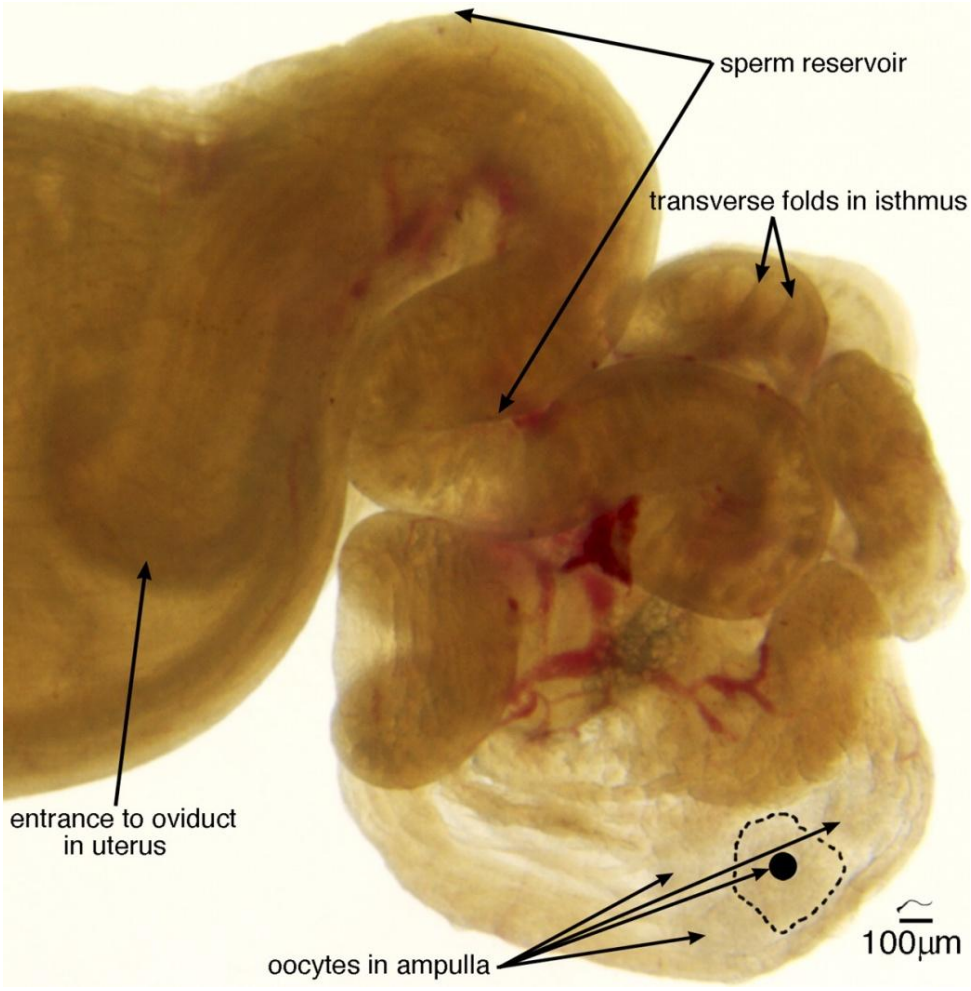

Figure 1.2. A transilluminated mouse oviduct. The ovary and bursa have been removed, but the coiling of the oviduct has been left in place. The size of mouse sperm (about 125 μm) is illustrated above the scale bar. The approximate location of the sperm reservoir is shown. In the sperm reservoir, the mucosal surface of the oviduct is thrown into transverse folds, creating pockets. These can be more clearly seen, as indicated by arrows, in the upper isthmus of the oviduct. To appreciate the size of the oocytes and cumulus in the ampulla, one oocyte has been covered by a solid black circle and the border of its cumulus indicated by a dotted line.

Mouse sperm provide an excellent model for understanding the response of the flagellum to the signals from a gradient of chemoattractant. This is because the hook-shaped head of the sperm enables one to distinguish the direction of the flagellar bend.

When the orientation of the flagellar bend is the same as that of the hook of the sperm head, the bend will be referred to as a "pro-hook" bend and when the flagellar bend is in the opposite orientation, it will be referred to as an "anti-hook" bend (Figure 1.3).

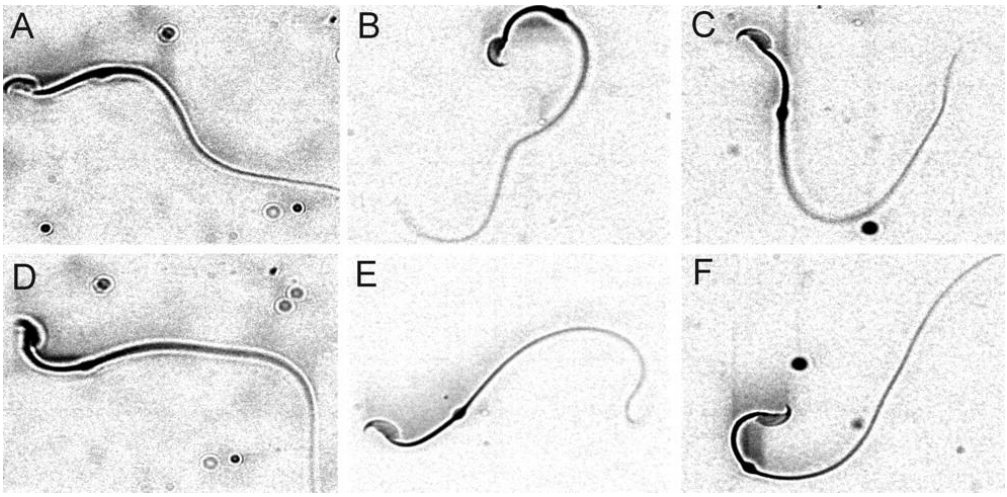

Figure 1.3. Flagellar beating patterns in mouse sperm. Activated (progressive) sperm show a symmetrical beating pattern, characterized by low amplitude pro-hook (**A**) and anti-hook (**D**) bends. Sperm hyperactivating under capacitating conditions show increased pro-hook bends (**B**), while the anti-hook bends remain unchanged (**E**). Sperm treated with thimerosal to release Ca^{2+} from internal stores show low-amplitude pro-hook bends (**C**) and high-amplitude anti-hook bends (**F**).

When mouse sperm are incubated under capacitating conditions until they hyperactivate, the pro-hook bend increases in amplitude, producing an asymmetrical beat pattern (see figures in Carlson *et al.* [28] and Fraser [78] and Figure 1.3). This response is due primarily to Ca^{2+} influx through CATSPER channels, because sperm from males lacking a functional CATSPER gene do not hyperactivate under capacitating conditions [21, 26, 28]. In contrast, when uncapacitated mouse sperm are treated with thimerosal to release Ca^{2+} from internal stores, the anti-hook bend increases in amplitude instead of the pro-hook bend (see movie in Marquez *et al.* [79]

and Figure 1.3). Capacitated sperm treated with thimerosal produce the same pattern as uncapacitated sperm (unpublished observations). This means that there are two types of asymmetrical beating; that is, dominant pro-hook beating, where the pro-hook bend is increased and dominant anti-hook beating, where the anti-hook bend is increased.

A study using a demembranated sperm model indicates that Ca^{2+} levels determine whether flagellar bend amplitude increases in a pro-hook or anti-hook direction. When rat sperm demembranated by detergent were reactivated with about 100 nM Ca^{2+}, the flagellum formed a bend in the pro-hook direction; however, when exposed to more than 2.5 μM Ca^{2+}, the flagellum formed an anti-hook bend [80]. It should be pointed out that demembranated rat sperm reactivated in micromolar Ca^{2+} become immotile after producing a single large anti-hook bend. Similarly, intact mouse sperm treated with thimerosal arrest in an anti-hook bend after five minutes of dominant anti-hook beating [79]. It is intriguing that mouse sperm treated with the odorant lyral also show this response, while sperm treated with the same amount of other floral odorants, bourgeonal or dihydromyrcenal, do not [54]. The arrest of motility is probably due to deleterious effects of prolonged elevation of cytosolic Ca^{2+}. However, if the RNE behaves like other intracellular Ca^{2+} stores, a physiologically triggered release of Ca^{2+} is likely to produce local high cytoplasmic Ca^{2+} levels that are rapidly reduced via removal from the cytoplasm by Ca^{2+}ATPase pumps and by Ca^{2+} uniporters in nearby mitochondria (reviewed by Berridge [81] and Clapham [82]). In sperm, the mitochondria at the base of the midpiece mitochondrial sheath lie

very close to the RNE [72] and thus could participate in rapid reduction of cytoplasmic Ca^{2+} (Figure 1.4). The momentary spike of Ca^{2+} might result in the momentary production of a large anti-hook bend without immobilizing the sperm. Just one large anti-hook bend would be sufficient to change the direction of the path of the sperm.

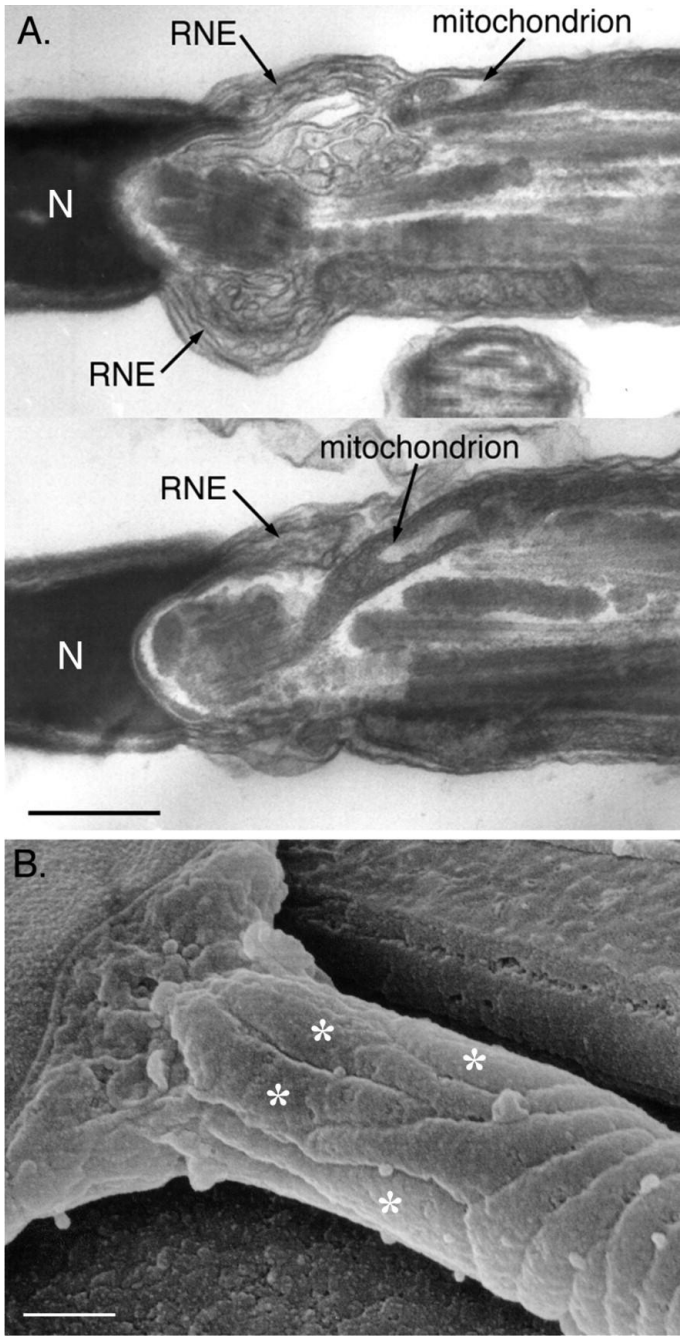

Figure 1.4. Transmission and scanning electron micrographs illustrate the close relationship of the redundant nuclear envelope (**RNE**) and mitochondria at the base of the flagellum. **A**) Transmission electron micrographs of the neck region of bull sperm. The nucleus is indicated by **N**. **B**) The asterisks indicate the mitochondria at the base of the flagellum. Note that they are unwound from the mitochondrial helix in the midpiece. The bars indicate 3 μm. Figure reprinted with permission [72].

The production of dominant pro-hook and dominant anti-hook beat patterns also indicates that the molecules or complexes with which Ca^{2+} interacts on one side or region of the flagellum have higher affinity for Ca^{2+} than those on the other side. Lindemann's group, which first reported the Ca^{2+} dependence of flagellar curvature in mammalian sperm, later demonstrated that Ni^{2+} and Cd^{2+} selectively block sliding of dynein along microtubules on one side of the flagellum, indicating differing sensitivities to divalent cations on the two sides of the flagellum that may reflect differing sensitivities to Ca^{2+} as well [83, 84].

The pattern of Ca^{2+} increase in the flagellum begins in the principal piece when CATSPER channels are stimulated, which is where the CATSPER channels are localized [21, 23, 85]. In contrast, when thapsigargin or thimerosal are used to stimulate release of Ca^{2+} from stores, the rise in Ca^{2+} initiates at the base of the flagellum, which is where the RNE is located. In both cases, the Ca^{2+} rise spreads along the flagellum, although from opposite directions. Thus, in addition to differences in cytoplasmic Ca^{2+} levels in the flagellum, the difference in the pattern of Ca^{2+} increase may also determine whether the pro-hook or anti-hook beat is dominant.

At this point, calmodulin is the only Ca^{2+}-binding protein known to play a role in Ca^{2+}-dependent modulation of the mammalian sperm flagellar beat by directly affecting the axoneme [86]. A testis-specific, Ca^{2+}-binding protein, CABYR, which interacts with A-kinase anchoring proteins (AKAPs), has been identified. It is localized in sperm flagella and tyrosine phosphorylated during *in vitro* capacitation, but its role in regulating sperm motility is unclear [87, 88]. There is evidence of

additional axoneme-associated Ca^{2+}-binding proteins in nonmammalian species. For example, a new member of the neuronal calcium sensor family, calaxin, has been shown to bind Ca^{2+} and associate with β tubulin and outer arm dynein in the flagella of sperm from the ascidian *Ciona intestinalis*. Potential homologs of calaxin have been identified in the mouse and human genomes [89]. Another protein, LC4, has been identified as a subunit of outer-arm dynein in *Chlamydomonas* and has been shown to undergo a conformation change in response to Ca^{2+} [90]. Additional Ca^{2+}-binding axonemal proteins may yet be discovered in mammalian sperm. If different Ca^{2+}-binding proteins are responsible for dominant pro-hook and dominant anti-hook flagellar beating, then these proteins should show different distributions in the axoneme.

In summary, we are proposing the following model for mammalian sperm. Hyperactivation is required for capacitated sperm to actively detach from the oviductal epithelium in order to move out of the storage reservoir. As hyperactivated sperm move up the oviduct, they become exposed to chemoattractants. A change in the concentration of chemoattractant modulates the dominant pro-hook beating pattern of hyperactivation, probably by inserting a single dominant anti-hook beat. This would manifest itself as a turn. Additional course-correcting turns could occur, with the final result of bringing sperm to the cumulus mass. The same chemoattractant, or additional chemoattractants, could similarly guide the sperm through the cumulus mass to the zona pellucida and oocyte.

Much remains to be learned about the regulatory mechanisms that bring sperm to the oocyte. Hopefully, the clues offered by the hook-shaped heads of rodent sperm will facilitate the elucidation of these mechanisms.

ACKNOWLEDGMENTS

The authors would like to thank C. Rose Gottlieb for drawing Figure 1.1.

REFERENCES

1. Yanagimachi R. The movement of golden hamster spermatozoa before and after capacitation. J Reprod Fertil 1970; 23:193-196.

2. Kaupp UB, Kashikar ND, Weyand I. Mechanisms of sperm chemotaxis. Annu Rev Physiol 2008; 70:93-117.

3. Schwartz R, Brooks W, Zinsser HH. Evidence of chemotaxis as a factor in sperm motility. Fertil Steril 1958; 9:300-308.

4. Dickmann Z. Chemotaxis of rabbit spermatozoa. J Exp Biol 1963; 40:1-5.

5. Villanueva-Diaz C, Vadillo-Ortega F, Kably-Ambe A, Diaz-Perez MA, Krivitzky SK. Evidence that human follicular fluid contains a chemoattractant for spermatozoa. Fertil Steril 1990; 54:1180-1182.

6. Ralt D, Goldenberg M, Fetterolf P, Thompson D, Dor J, Mashiach S, Garbers DL, Eisenbach M. Sperm attraction to a follicular factor(s) correlates with human egg fertilizability. Proc Natl Acad Sci U S A 1991; 88:2840-2844.

7. Ralt D, Manor M, Cohen-Dayag A, Tur-Kaspa I, Ben-Shlomo I, Makler A, Yuli I, Dor J, Blumberg S, Mashiach S, et al. Chemotaxis and chemokinesis of human spermatozoa to follicular factors. Biol Reprod 1994; 50:774-785.

8. Eisenbach M, Giojalas LC. Sperm guidance in mammals - an unpaved road to

the egg. Nat Rev Mol Cell Biol 2006; 7:276-285.

9. Carlson AE, Hille B, Babcock DF. External Ca2+ acts upstream of adenylyl cyclase SACY in the bicarbonate signaled activation of sperm motility. Dev Biol 2007; 312:183-192.

10. Eddy EM. The spermatozoon. In: Neill JD (ed), The Physiology of Reproduction, vol 1, 3 rd ed. New York: Academic Press; 2006: 3-54.

11. Wennemuth G, Carlson AE, Harper AJ, Babcock DF. Bicarbonate actions on flagellar and Ca2+ -channel responses: initial events in sperm activation. Development 2003; 130:1317-1326.

12. Spehr M, Schwane K, Riffell JA, Barbour J, Zimmer RK, Neuhaus EM, Hatt H. Particulate adenylate cyclase plays a key role in human sperm olfactory receptor-mediated chemotaxis. J Biol Chem 2004; 279:40194-40203.

13. Gakamsky A, Schechtman E, Caplan SR, Eisenbach M. Analysis of chemotaxis when the fraction of responsive cells is small--application to mammalian sperm guidance. Int J Dev Biol 2008; 52:481-487.

14. Suarez SS, Pacey AA. Sperm transport in the female reproductive tract. Hum Reprod Update 2006; 12:23-37.

15. Suarez SS, Osman RA. Initiation of hyperactivated flagellar bending in mouse sperm within the female reproductive tract. Biol Reprod 1987; 36:1191-1198.

16. DeMott RP, Suarez SS. Hyperactivated sperm progress in the mouse oviduct. Biol Reprod 1992; 46:779-785.

17. Pacey AA, Davies N, Warren MA, Barratt CL, Cooke ID. Hyperactivation may assist human spermatozoa to detach from intimate association with the endosalpinx. Hum Reprod 1995; 10:2603-2609.

18. Ho K, Wolff CA, Suarez SS. CatSper-null mutant spermatozoa are unable to ascend beyond the oviductal reservoir. Reprod Fertil Dev 2009; 21:345-350.

19. Suarez SS, Katz DF, Owen DH, Andrew JB, Powell RL. Evidence for the function of hyperactivated motility in sperm. Biol Reprod 1991; 44:375-381.

20. Suarez SS, Dai X. Hyperactivation enhances mouse sperm capacity for penetrating viscoelastic media. Biol Reprod 1992; 46:686-691.

21. Quill TA, Sugden SA, Rossi KL, Doolittle LK, Hammer RE, Garbers DL. Hyperactivated sperm motility driven by CatSper2 is required for fertilization. Proc Natl Acad Sci U S A 2003; 100:14869-14874.

22. Stauss CR, Votta TJ, Suarez SS. Sperm motility hyperactivation facilitates penetration of the hamster zona pellucida. Biol Reprod 1995; 53:1280-1285.

23. Ren D, Navarro B, Perez G, Jackson AC, Hsu S, Shi Q, Tilly JL, Clapham DE. A sperm ion channel required for sperm motility and male fertility. Nature 2001; 413:603-609.

24. Quill TA, Ren D, Clapham DE, Garbers DL. A voltage-gated ion channel expressed specifically in spermatozoa. Proc Natl Acad Sci U S A 2001; 98:12527-12531.

25. Overstreet JW, Cooper GW. Effect of ovulation and sperm motility on the migration of rabbit spermatozoa to the site of fertilization. J Reprod Fertil 1979; 55:53-59.

26. Carlson AE, Quill TA, Westenbroek RE, Schuh SM, Hille B, Babcock DF. Identical phenotypes of CatSper1 and CatSper2 null sperm. J Biol Chem 2005; 280:32238-32244.

27. Qi H, Moran MM, Navarro B, Chong JA, Krapivinsky G, Krapivinsky L, Kirichok Y, Ramsey IS, Quill TA, Clapham DE. All four CatSper ion channel proteins are required for male fertility and sperm cell hyperactivated motility. Proc Natl Acad Sci U S A 2007; 104:1219-1223.

28. Carlson AE, Westenbroek RE, Quill T, Ren D, Clapham DE, Hille B, Garbers DL, Babcock DF. CatSper1 required for evoked Ca2+ entry and control of flagellar function in sperm. Proc Natl Acad Sci U S A 2003; 100:14864-14868.

29. Navarro B, Kirichok Y, Chung JJ, Clapham DE. Ion channels that control fertility in mammalian spermatozoa. Int J Dev Biol 2008; 52:607-613.

30. Maas DH, Storey BT, Mastroianni L, Jr. Hydrogen ion and carbon dioxide content of the oviductal fluid of the rhesus monkey (Macaca mulatta). Fertil Steril 1977; 28:981-985.

31. Eisenbach M. Sperm chemotaxis. Rev Reprod 1999; 4:56-66.

32. Matsumoto M, Briones AV, Nishigaki T, Hoshi M. Sequence analysis of cDNAs encoding precursors of starfish asterosaps. Dev Genet 1999; 25:130-136.

33. Garbers DL. Molecular basis of fertilization. Annu Rev Biochem 1989; 58:719-742.

34. Suzuki N. Structure, function and biosynthesis of sperm-activating peptides

and fucose sulfate glycoconjugate in the extracellular coat of sea urchin eggs. Zoolog Sci 1995; 12:13-27.

35. Sun F, Giojalas LC, Rovasio RA, Tur-Kaspa I, Sanchez R, Eisenbach M. Lack of species-specificity in mammalian sperm chemotaxis. Dev Biol 2003; 255:423-427.

36. Cohen-Dayag A, Tur-Kaspa I, Dor J, Mashiach S, Eisenbach M. Sperm capacitation in humans is transient and correlates with chemotactic responsiveness to follicular factors. Proc Natl Acad Sci U S A 1995; 92:11039-11043.

37. Fabro G, Rovasio RA, Civalero S, Frenkel A, Caplan SR, Eisenbach M, Giojalas LC. Chemotaxis of capacitated rabbit spermatozoa to follicular fluid revealed by a novel directionality-based assay. Biol Reprod 2002; 67:1565-1571.

38. Wang Y, Storeng R, Dale PO, Abyholm T, Tanbo T. Effects of follicular fluid and steroid hormones on chemotaxis and motility of human spermatozoa in vitro. Gynecol Endocrinol 2001; 15:286-292.

39. Sun F, Bahat A, Gakamsky A, Girsh E, Katz N, Giojalas LC, Tur-Kaspa I, Eisenbach M. Human sperm chemotaxis: both the oocyte and its surrounding cumulus cells secrete sperm chemoattractants. Hum Reprod 2005; 20:761-767.

40. Tamba S, Yodoi R, Segi-Nishida E, Ichikawa A, Narumiya S, Sugimoto Y. Timely interaction between prostaglandin and chemokine signaling is a prerequisite for successful fertilization. Proc Natl Acad Sci U S A 2008; 105:14539-14544.

41. Oren-Benaroya R, Orvieto R, Gakamsky A, Pinchasov M, Eisenbach M. The sperm chemoattractant secreted from human cumulus cells is progesterone. Hum Reprod 2008; 23:2339-2345.

42. Guidobaldi HA, Teves ME, Unates DR, Anastasia A, Giojalas LC. Progesterone from the cumulus cells is the sperm chemoattractant secreted by the rabbit oocyte cumulus complex. PLoS One 2008; 3:e3040.

43. Osman RA, Andria ML, Jones AD, Meizel S. Steroid induced exocytosis: the human sperm acrosome reaction. Biochem Biophys Res Commun 1989; 160:828-833.

44. Teves ME, Barbano F, Guidobaldi HA, Sanchez R, Miska W, Giojalas LC. Progesterone at the picomolar range is a chemoattractant for mammalian spermatozoa. Fertil Steril 2006; 86:745-749.

45. Harper CV, Barratt CL, Publicover SJ. Stimulation of human spermatozoa with progesterone gradients to simulate approach to the oocyte. Induction of [Ca(2+)](i) oscillations and cyclical transitions in flagellar beating. J Biol Chem 2004; 279:46315-46325.

46. Teves ME, Guidobaldi HA, Unates DR, Sanchez R, Miska W, Publicover SJ, Morales Garcia AA, Giojalas LC. Molecular mechanism for human sperm chemotaxis mediated by progesterone. PLoS One 2009; 4:e8211.

47. Jaiswal BS, Tur-Kaspa I, Dor J, Mashiach S, Eisenbach M. Human sperm chemotaxis: is progesterone a chemoattractant? Biol Reprod 1999; 60:1314-1319.

48. Roldan ER, Murase T, Shi QX. Exocytosis in spermatozoa in response to progesterone and zona pellucida. Science 1994; 266:1578-1581.

49. Murase T, Roldan ER. Progesterone and the zona pellucida activate different transducing pathways in the sequence of events leading to diacylglycerol generation during mouse sperm acrosomal exocytosis. Biochem J 1996; 320 (Pt 3):1017-1023.

50. Schuffner AA, Bastiaan HS, Duran HE, Lin ZY, Morshedi M, Franken DR, Oehninger S. Zona pellucida-induced acrosome reaction in human sperm: dependency on activation of pertussis toxin-sensitive G(i) protein and extracellular calcium, and priming effect of progesterone and follicular fluid. Mol Hum Reprod 2002; 8:722-727.

51. Vanderhaeghen P, Schurmans S, Vassart G, Parmentier M. Olfactory receptors are displayed on dog mature sperm cells. J Cell Biol 1993; 123:1441-1452.

52. Walensky LD, Roskams AJ, Lefkowitz RJ, Snyder SH, Ronnett GV. Odorant receptors and desensitization proteins colocalize in mammalian sperm. Mol Med 1995; 1:130-141.

53. Spehr M, Gisselmann G, Poplawski A, Riffell JA, Wetzel CH, Zimmer RK, Hatt H. Identification of a testicular odorant receptor mediating human sperm chemotaxis. Science 2003; 299:2054-2058.

54. Fukuda N, Yomogida K, Okabe M, Touhara K. Functional characterization of a mouse testicular olfactory receptor and its role in chemosensing and in regulation of sperm motility. J Cell Sci 2004; 117:5835-5845.

55. Yanagimachi R, Usui N. Calcium dependence of the acrosome reaction and activation of guinea pig spermatozoa. Exp Cell Res 1974; 89:161-174.

56. Neill JM, Olds-Clarke P. A computer-assisted assay for mouse sperm hyperactivation demonstrates that bicarbonate but not bovine serum albumin is required. Gamete Res 1987; 18:121-140.

57. Suarez SS, Vincenti L, Ceglia MW. Hyperactivated motility induced in mouse sperm by calcium ionophore A23187 is reversible. J Exp Zool 1987; 244:331-336.

58. Suarez SS, Dai XB, DeMott RP, Redfern K, Mirando MA. Movement characteristics of boar sperm obtained from the oviduct or hyperactivated in vitro. J Androl 1992; 13:75-80.

59. Marquez B, Suarez SS. Bovine sperm hyperactivation is promoted by alkaline-stimulated Ca2+ influx. Biol Reprod 2007; 76:660-665.

60. Suarez SS, Varosi SM, Dai X. Intracellular calcium increases with hyperactivation in intact, moving hamster sperm and oscillates with the flagellar beat cycle. Proc Natl Acad Sci U S A 1993; 90:4660-4664.

61. Suarez SS, Dai X. Intracellular calcium reaches different levels of elevation in hyperactivated and acrosome-reacted hamster sperm. Mol Reprod Dev 1995; 42:325-333.

62. Ho HC, Granish KA, Suarez SS. Hyperactivated motility of bull sperm is triggered at the axoneme by Ca2+ and not cAMP. Dev Biol 2002; 250:208-217.

63. Publicover SJ, Giojalas LC, Teves ME, de Oliveira GS, Garcia AA, Barratt CL, Harper CV. Ca2+ signalling in the control of motility and guidance in mammalian sperm. Front Biosci 2008; 13:5623-5637.

64. Suarez SS. Control of hyperactivation in sperm. Hum Reprod Update 2008; 14:647-657.

65. Carlson AE, Burnett LA, del Camino D, Quill TA, Hille B, Chong JA, Moran MM, Babcock DF. Pharmacological targeting of native CatSper channels reveals a required role in maintenance of sperm hyperactivation. PLoS One 2009; 4:e6844.

66. Castellano LE, Trevino CL, Rodriguez D, Serrano CJ, Pacheco J, Tsutsumi V, Felix R, Darszon A. Transient receptor potential (TRPC) channels in human sperm: expression, cellular localization and involvement in the regulation of flagellar motility. FEBS Lett 2003; 541:69-74.

67. Wiesner B, Weiner J, Middendorff R, Hagen V, Kaupp UB, Weyand I. Cyclic

nucleotide-gated channels on the flagellum control Ca2+ entry into sperm. J Cell Biol 1998; 142:473-484.

68. Darszon A, Acevedo JJ, Galindo BE, Hernandez-Gonzalez EO, Nishigaki T, Trevino CL, Wood C, Beltran C. Sperm channel diversity and functional multiplicity. Reproduction 2006; 131:977-988.

69. Ho HC, Suarez SS. Characterization of the intracellular calcium store at the base of the sperm flagellum that regulates hyperactivated motility. Biol Reprod 2003; 68:1590-1596.

70. Lytton J, Westlin M, Hanley MR. Thapsigargin inhibits the sarcoplasmic or endoplasmic reticulum Ca-ATPase family of calcium pumps. J Biol Chem 1991; 266:17067-17071.

71. Elferink JG. Thimerosal: a versatile sulfhydryl reagent, calcium mobilizer, and cell function-modulating agent. Gen Pharmacol 1999; 33:1-6.

72. Ho HC, Suarez SS. An inositol 1,4,5-trisphosphate receptor-gated intracellular Ca(2+) store is involved in regulating sperm hyperactivated motility. Biol Reprod 2001; 65:1606-1615.

73. Ward GE, Brokaw CJ, Garbers DL, Vacquier VD. Chemotaxis of Arbacia punctulata spermatozoa to resact, a peptide from the egg jelly layer. J Cell Biol 1985; 101:2324-2329.

74. Shiba K, Baba SA, Inoue T, Yoshida M. Ca2+ bursts occur around a local minimal concentration of attractant and trigger sperm chemotactic response. Proc Natl Acad Sci U S A 2008; 105:19312-19317.

75. Bohmer M, Van Q, Weyand I, Hagen V, Beyermann M, Matsumoto M, Hoshi M, Hildebrand E, Kaupp UB. Ca2+ spikes in the flagellum control chemotactic behavior of sperm. Embo J 2005; 24:2741-2752.

76. Spehr M, Schwane K, Riffell JA, Zimmer RK, Hatt H. Odorant receptors and olfactory-like signaling mechanisms in mammalian sperm. Mol Cell Endocrinol 2006; 250:128-136.

77. Suarez SS. Regulation of sperm storage and movement in the mammalian oviduct. Int J Dev Biol 2008; 52:455-462.

78. Fraser LR. Motility patterns in mouse spermatozoa before and after capacitation. J Exp Zool 1977; 202:439-444.

79. Marquez B, Ignotz G, Suarez SS. Contributions of extracellular and

intracellular Ca2+ to regulation of sperm motility: Release of intracellular stores can hyperactivate CatSper1 and CatSper2 null sperm. Dev Biol 2007; 303:214-221.

80. Lindemann CB, Goltz JS. Calcium regulation of flagellar curvature and swimming pattern in triton X-100--extracted rat sperm. Cell Motil Cytoskeleton 1988; 10:420-431.

81. Berridge MJ. Calcium microdomains: organization and function. Cell Calcium 2006; 40:405-412.

82. Clapham DE. Calcium signaling. Cell 2007; 131:1047-1058.

83. Kanous KS, Casey C, Lindemann CB. Inhibition of microtubule sliding by Ni2+ and Cd2+: evidence for a differential response of certain microtubule pairs within the bovine sperm axoneme. Cell Motil Cytoskeleton 1993; 26:66-76.

84. Lindemann CB, Walker JM, Kanous KS. Ni2+ inhibition induces asymmetry in axonemal functioning and bend initiation of bull sperm. Cell Motil Cytoskeleton 1995; 30:8-16.

85. Xia J, Reigada D, Mitchell CH, Ren D. CATSPER channel-mediated Ca2+ entry into mouse sperm triggers a tail-to-head propagation. Biol Reprod 2007; 77:551-559.

86. Ignotz GG, Suarez SS. Calcium/calmodulin and calmodulin kinase II stimulate hyperactivation in demembranated bovine sperm. Biol Reprod 2005; 73:519-526.

87. Naaby-Hansen S, Mandal A, Wolkowicz MJ, Sen B, Westbrook VA, Shetty J, Coonrod SA, Klotz KL, Kim YH, Bush LA, Flickinger CJ, Herr JC. CABYR, a novel calcium-binding tyrosine phosphorylation-regulated fibrous sheath protein involved in capacitation. Dev Biol 2002; 242:236-254.

88. Newell AE, Fiedler SE, Ruan JM, Pan J, Wang PJ, Deininger J, Corless CL, Carr DW. Protein kinase A RII-like (R2D2) proteins exhibit differential localization and AKAP interaction. Cell Motil Cytoskeleton 2008; 65:539-552.

89. Mizuno K, Padma P, Konno A, Satouh Y, Ogawa K, Inaba K. A novel neuronal calcium sensor family protein, calaxin, is a potential Ca(2+)-dependent regulator for the outer arm dynein of metazoan cilia and flagella. Biol Cell 2009; 101:91-103.

90. Sakato M, Sakakibara H, King SM. Chlamydomonas outer arm dynein alters

conformation in response to Ca2+. Mol Biol Cell 2007; 18:3620-3634.

CHAPTER 2

Two Distinct Ca^{2+} Signaling Pathways Modulate Sperm Flagellar Beating Patterns in Mice*

ABSTRACT

Hyperactivation, a swimming pattern of mammalian sperm in the oviduct, is essential for fertilization. It is characterized by asymmetrical flagellar beating and an increase of cytoplasmic Ca^{2+}. We observed that some mouse sperm swimming in the oviduct produce high-amplitude pro-hook bends (bends in the direction of the hook on the head), whereas other sperm produce high-amplitude anti-hook bends. Switching direction of the major bends could serve to redirect sperm toward oocytes. We hypothesized that different Ca^{2+} signaling pathways produce high-amplitude pro-hook and anti-hook bends. In vitro, sperm that hyperactivated during capacitation (because of activation of CATSPER plasma membrane Ca^{2+} channels) developed high-amplitude pro-hook bends. The CATSPER activators procaine and 4-aminopyridine (4-AP) also induced high-amplitude pro-hook bends. Thimerosal, which triggers a Ca^{2+} release from internal stores, induced high-amplitude anti-hook bends. Activation of CATSPER channels is facilitated by a pH rise, so both Ca^{2+} and pH responses to treatments with 4-AP and thimerosal were monitored. Thimerosal triggered a

---

*Chang H, Suarez SS. Two distinct Ca^{2+} signaling pathways modulate sperm flagellar beating patterns in mice. Biol Reprod 2011; 85:296-305.

Ca^{2+} increase that initiated at the base of the flagellum, whereas 4-AP initiated a rise in the proximal principal piece. Only 4-AP triggered a flagellar pH rise. Proteins were extracted from sperm for examination of phosphorylation patterns induced by Ca^{2+} signaling. Procaine and 4-AP induced phosphorylation of proteins on threonine and serine, whereas thimerosal primarily induced dephosphorylation of proteins. Tyrosine phosphorylation was unaffected. We concluded that hyperactivation, which is associated with capacitation, can be modulated by release of Ca^{2+} from intracellular stores to reverse the direction of the dominant flagellar bend and, thus, redirect sperm.

INTRODUCTION

In the oviduct, mammalian sperm enter a state of vigorous flagellar beating known as hyperactivation. Hyperactivation is a swimming pattern characterized by high-amplitude, asymmetrical flagellar beating, resulting in circular or helical swimming trajectories when sperm are placed on glass slides [1]. This contrasts with the activated motility of sperm in the ejaculate, which is characterized by low-amplitude, symmetrical flagellar beating, resulting in a progressive and linear swimming pattern. Hyperactivation is generally considered to be a part of capacitation, which is a network of processes that sperm must undergo to be able to fertilize oocytes (for review, see [2]).

Evidence exists that hyperactivation plays various roles in the oviduct. First, sperm use hyperactivation to detach from the oviductal epithelium to escape from the oviductal storage reservoir (for review, see [3]; see also [4–7]). Second, hyperactivation provides sperm with a greater thrusting force to swim through oviductal mucus and to penetrate the viscoelastic cumulus matrix surrounding the oocyte [8–10]. Third, hyperactivation is required by sperm to penetrate the zona pellucida of the oocyte to reach and fuse with the oocyte plasma membrane [11–13].

The critical importance of hyperactivation to fertilization was confirmed with the discovery of CATSPER channels. CATSPER channels are pH-sensitive, voltage-dependent Ca^{2+} channels specific to male germ cells. CATSPER channels are located in the plasma membrane of the principal piece of the flagellum [12, 13]. CATSPER-

null male mice are infertile, primarily because their sperm are unable to hyperactivate (for reviews, see [14–16]).

Even though hyperactivation assists sperm in reaching oocytes, the circumstances under which fertilization occurs suggest that hyperactivation must be modulated to enable successful fertilization. In rabbits and mice, hyperactivation begins in the lower oviduct [5,17], and this enables mouse sperm to escape from the sperm storage reservoir [5, 7]. This region is quite far from the site of fertilization; in mice, a long length of coiled oviduct separates the reservoir from the ampulla where fertilization occurs. Furthermore, mouse oocytes are buried deeply within a large cumulus oophorus. It seems unlikely that a hyperactivated sperm could reach an oocyte without adjusting its trajectory periodically. Therefore, the flagellar beating of hyperactivated sperm very likely is modulated, at least intermittently, to redirect the sperm toward the oocyte.

Mouse sperm provide an excellent model for understanding the modulation of flagellar bending during hyperactivation, because the hook-shaped head of the sperm enables one to determine the direction of the flagellar bend. In reviewing videotapes of sperm swimming in the oviduct, we observed that some sperm produced high-amplitude pro-hook bends, whereas others produced high-amplitude anti-hook bends.

The Ca^{2+} signaling plays an important role in determining the pattern of the flagellar beat, especially during hyperactivation. Although the factors that initiate hyperactivation remain elusive, strong evidence indicates that a rise in flagellar Ca^{2+} is

necessary for hyperactivation (for review, see [16]). The predominant source of Ca^{2+} is extracellular Ca^{2+}, which enters the flagellum primarily through CATSPER channels (for review, see [14–16]; see also [18]). In addition, Ca^{2+} may be provided by a Ca^{2+} store in the redundant nuclear envelope (RNE) that lies at the base of the flagellum. Treatment of sperm with thimerosal [19] or thapsigargin [20], which stimulate release of Ca^{2+} from stores, raises flagellar Ca^{2+} and produces asymmetrical flagellar beating resembling hyperactivation [21]; however, preliminary observations of mouse sperm indicate that the response is actually the reverse of hyperactivation—that is, the high-amplitude bends form in the anti-hook direction [22]. We recently proposed that switching the dominant flagellar bend from the pro-hook to the anti-hook side modulates hyperactivation and redirects the path of the sperm [23]. Therefore, in the present study, we tested the hypothesis that different Ca^{2+}signaling pathways induce dominant pro-hook and dominant anti-hook bending. To do this, we compared the patterns of Ca^{2+} rise, pH rise, and protein phosphorylation in sperm treated to activate plasma membrane CATSPER channels with those of sperm treated to release $Ca^{2+}$from internal stores.

MATERIALS AND METHODS

Media and Chemicals

All routine chemicals and compounds were purchased from Sigma-Aldrich Co. with the exceptions noted below. A mouse sperm capacitating medium [4] was used for incubating and washing sperm. The medium consisted of 110 mM NaCl, 2.68 mM KCl, 0.36 mM NaH_2PO_4, 25 mM $NaHCO_3$, 25 mM Hepes (EMD Chemicals), 5.56 mM glucose, 1.0 mM pyruvic acid, 0.006% penicillin G (Na), 2.4 mM $CaCl_2$, and 0.49 mM $MgCl_2$. It also included 10 mg/ml of bovine serum albumin (BSA; EMD Chemicals) except when otherwise specified. The osmolarity range was 290-310 mOsm/kg and the pH was adjusted to 7.6.

Animals

A hybrid cross (C57BL/6J ×BALB/cByJ) of wild-type F_1 males aged 3–6 mo were obtained from Dr. John Schimenti (Cornell University, Department of Biomedical Sciences). The F_1 hybrids produced sperm of consistently high quality in terms of morphology and fertility, more so than outbred strains such as CD1. Mice were euthanized by CO_2 inhalation. All procedures were approved by the Institutional Animal Care and Use Committee at Cornell University.

Sperm Preparation and Hyperactivation

Sperm were obtained from freshly dissected epididymides as follows: A 100-µl droplet of medium was covered by mineral oil in a 35- ×10-mm Petri dish (Falcon),

which was equilibrated in an incubator at 37 ℃ and 5% CO_2 before use. Caudal epididymides were cleaned of fat, and then blood was gently pushed out of surface vessels. The caudal epididymides were placed under the mineral oil in the Petri dish. Several cuts were made in the coiled tubules near the vas deferens, and the emerging thick fluid containing sperm was gently pulled out of each cut using no. 5 tweezers and then transferred under the oil to the droplet of medium. Sperm were allowed to disperse for 10 min in the incubator, and samples were counted using a hemocytometer. Then, sperm were diluted with medium to 5×10^6 sperm/ml and used immediately.

Immediately after dilution in medium, sperm were treated with 5 mM procaine for 4 min or with 4 mM 4-aminopyridine (4-AP; Tocris Bioscience) for 1 min [22, 24, 25] to activate CATSPER channels or with the inositol trisphosphate (IP_3) receptor agonist thimerosal (100 μM) for 30 sec [19] to stimulate release of Ca^{2+} from stores. As a negative control, medium alone was added to sperm, which were then incubated for 4 min. In addition, 500-μl aliquots of sperm were incubated in medium at 37 ℃ under 5% CO_2 for 2 h to promote capacitation.

To examine the combined effects of the pharmacological agents, sperm that achieved maximal responses when treated with procaine or 4-AP, or when incubated under capacitating conditions for 2 h, were treated with 100 μM thimerosal for 30 sec. Sperm were also treated with thimerosal to achieve maximal response first, then treated with procaine or 4-AP as described above.

Analysis of Sperm Motility

Samples of sperm were placed on slides on a 37 ℃ stage of a Zeiss Axiovert 35 microscope and videotaped using bright-field microscopy with a 20 × objective and a Dage CCD 72 video camera (Dage-MTI, Inc.) connected to a Panasonic AG-1970 Super VHS videocassette recorder (Panasonic Industrial Co.). Playback of the videotapes was used to determine the percentages of motile sperm (i.e., sperm showing any type of flagellar activity) and of sperm swimming in various patterns. For each sample, 100–120 motile sperm were analyzed, and for each experiment, replicate tests were performed using samples from three males.

Intracellular Ca^{2+} and pH Detection

Sperm (5×10^6 sperm/ml) were loaded by incubation with the Ca^{2+} indicator Fluo-4 AM (10 μM; Invitrogen) or the acetoxymethyl (AM) ester derivative of the pH-sensitive dye 2′,7′-bis-(2-carboxyethyl)-5-(and-6)-carboxyfluorescein (BCECF-AM; 5 μM; Invitrogen) for 30 min in BSA-free medium. Extracellular dye was removed by centrifugation at 170 × *g* for 5 min. For the 4-AP treatment, Fluo-4 AM-loaded sperm were resuspended in BSA-free medium and incubated for an additional 30 min to allow de-esterification of the dye into its membrane-impermeable, Ca^{2+}-sensitive form. For thimerosal treatment, dye-loaded sperm were resuspended in BSA- and Ca^{2+}-free medium to produce a final concentration of 30 μM Ca^{2+} and incubated for 30 min to allow de-esterification [21]. Sperm loaded with BCECF-AM were resuspended in

BSA-free medium to de-esterify for 30 min into its membrane-impermeable, pH-sensitive form. All incubations were performed in an incubator at 37 ℃ under 5% CO_2 in humidified air.

To examine fluorescence patterns, aliquots of sperm suspension were transferred to glass-bottom wells in a 96-well plate (In Vitro Scientific). The glass bottoms had been coated with Cell-Tak (BD Biosciences), which caused sperm to adhere to the glass bottom. The fluorescence of individual sperm was monitored before and after application of treatments. The temperature was maintained at 37 ℃ throughout each experiment. Fluorescence intensity was detected using a 480- ± 40-nm excitation filter, a 535- ± 50-nm emission filter, and a 505-nm long-pass dichroic mirror (Chroma Technology Corp.) with an oil-immersion, 100 × Fluar objective (N.A. 1.3; Carl Zeiss, Inc.). Stroboscopic illumination was provided by a 75-W xenon arc flash lamp (Chadwick-Helmuth Co.). Images were captured with a sensicam em high-performance camera (The Cooke Corporation) at 4 frames/sec controlled by IPLab Spectrum software (Version 4.0; Signal Analytics). Data for each treatment were collected from 15 to 20 sperm/mouse, and the experiments were replicated three times, each time with sperm from a different mouse.

The fluorescence of pH in sperm populations was also monitored before and after treatments using a Bio-Tek Synergy 2 kinetic microplate reader. Sperm loaded with BCECF-AM were placed in wells of a prewarmed, 96-well, black-bottom plate (Thermo Fisher Scientific). Each well contained 200000 sperm. Samples were analyzed immediately on the plate reader at an excitation wavelength of 490 nm and

an emission wavelength of 535 nm. The fluorescence dynamics were recorded every 3 sec. Readings for each time point were normalized, averaged, and expressed as relative fluorescence units. The procedure was repeated using sperm from a total of three mice.

Acrosome Reaction Analysis

Coomassie blue staining [26] was used to determine if the procaine, 4-AP, or thimerosal treatments induced acrosome reactions. As a positive control, the Ca^{2+} ionophore A23187 (20 μM) was used to treat sperm for 15 min to induce acrosome reactions. Treated sperm were fixed in 4% paraformaldehyde for 10 min and washed with PBS by centrifuging at 700 $\times g$ for 3 min. The sperm pellet was resuspended in 0.1 M ammonium acetate (pH 9) and dried on microscope slides. The sperm were stained with 0.22% Brilliant Blue G for 2 min. Excess stain was rinsed off with PBS. Slides were mounted using Permount (Fisher Scientific) and examined using bright-field optics at 400×. At least 100 sperm were examined for acrosomal status for each treatment. Samples from three mice were evaluated.

One-Dimensional Gel Electrophoresis and Western Blot Analysis

Aliquots of 1×10^6 sperm were treated with procaine, 4-AP, thimerosal, or medium control or were incubated under capacitating conditions as described above,

and then protease (Complete, EDTA-free; Roche) and phosphatase (PhosStop; Roche) inhibitors were added and the sperm collected by centrifugation at 1900 $\times g$ for 10 min at 4 ℃. The sperm pellet was solubilized in an SDS lysis buffer with 5% 2-mercaptoethanol and boiled for 5 min. Lysates were centrifuged to remove insoluble material and resolved by SDS–PAGE. The resolved proteins were transferred to polyvinylidene fluoride (PVDF) membranes (Millipore), and then the membranes were blocked for 1 h in Tris-buffered saline containing 0.05% Tween 20 (TTBS) and 5% gelatin from cold-water fish skin (G7765; Sigma). Tyrosine-phosphorylated proteins were detected by incubating overnight at 4 ℃ with 0.1 μg/ml of monoclonal antiphosphotyrosine antibody (05321; Millipore). Horseradish peroxidase (HRP)-conjugated goat anti-rabbit immunoglobulin G (1:10000; Sigma) and enhanced chemiluminescence (SuperSignal West Pico; Pierce) were used to visualize antibody-labeled proteins.

Two-Dimensional Gel Electrophoresis and Western Blot Analysis

Aliquots of 5 $\times 10^6$ sperm were treated with procaine, 4-AP, thimerosal, or medium control or sperm were incubated under capacitating conditions as described above, and then protease and phosphatase inhibitors were added and the sperm collected by centrifugation at 1900 $\times g$ for 10 min at 4 ℃. The sperm pellet was solubilized in a lysis buffer containing 7 M urea (EMD Chemicals), 2 M thiourea, 1% 3-(4-Heptyl)phenyl-3-hydroxypropyl)dimethylammoniopropanesulfonate (C7BzO;

Sigma), 50 mM dithiothreitol (DTT; Pierce) and 0.2% Ampholine (pH 3–10; Fluka) at room temperature for 1 h. Lysates were centrifuged to remove insoluble material.

For the first dimension of two-dimensional gel electrophoresis, IPG strips (7 cm, pH 3–10 nonlinear; Bio-Rad) were rehydrated with 125 μl of protein lysate for 14 h at 50 V and then focused at 4000 V for 2.5 h. After equilibration of the IPG strips in 125 mM Tris, 6 M urea, 10% glycerol, 2% SDS, and 4% DTT (pH 6.8), second-dimension SDS-PAGE gels were run and then transferred to PVDF membranes. Membranes were blocked for 1 h with 5% gelatin from cold-water fish skin in TTBS. Phosphoserine- and phosphothreonine-containing proteins were detected by incubating overnight at 4°C with 0.25 μg/ml (1:1000) of antiphosphoserine (AB1603; Millipore) or antiphosphothreonine (AB1607; Millipore) rabbit polyclonal antibodies diluted in TTBS containing 2% normal goat serum (EMD Chemicals). HRP-conjugated secondary antibodies (1:10000; Sigma) and enhanced chemiluminescence were used to visualize target proteins. Blots were stripped by the Restore Western Blot stripping buffer (Thermo Scientific) and then reprobed with the next antibody. Equal protein loading was verified with MemCode Reversible Protein Stain kit (Thermo Scientific) after the Western blot analysis.

Immunocytochemistry

Sperm treated with procaine, 4-AP, thimerosal, or medium control were fixed by 1% paraformaldehyde in PBS with gentle agitation for 15 min at room temperature.

Fixed sperm were collected by centrifugation at 700 $\times g$ for 3 min and then resuspended in 0.2 M glycine in PBS to quench residual fixative and agitated for 15 min at room temperature. Sperm were then either concentrated by centrifugation or diluted with PBS to give a final concentration of 5×10^6 sperm/ml. Samples of 10 μl were spotted onto ethanol-cleaned microscope slides and allowed to dry at room temperature overnight. Sperm smears were permeabilized with cold methanol for 10 min and then rinsed with PBS (three times for 5 min each time). Then, sperm were blocked with 3% BSA in PBS for 1 h. Antiphosphoserine (0.5 μg/ml, 1:500) or antiphosphothreonine (0.5 μg/ml, 1:500) antibodies were added, and the slides were incubated for 1 h at room temperature. The secondary antibody, goat-anti-rabbit fluorescein isothiocyanate (F9887; Sigma), was used at a dilution of 1:200.

Statistical Analysis

In motility studies, the percentages of sperm showing dominant pro-hook and anti-hook beating patterns were normalized using arcsin square root transformation and were compared using the paired Student *t*-test with Bonferroni corrections made for multiple comparisons. For assessing acrosome reactions, the percentage data were normalized using arcsin square root transformation and were analyzed using one-way ANOVA to test for statistically significant differences among treatments, followed by a Tukey honestly significant difference pairwise comparison test using VassarStats online software (http://faculty.vassar.edu/lowry/VassarStats.html).

RESULTS

Pharmacological Agents Induced High-Amplitude Pro-Hook or Anti-Hook Flagellar Bending

Analysis of video-recorded images of free-swimming sperm revealed that after 2 h of incubation under capacitating conditions, sperm predominantly showed high-amplitude pro-hook flagellar beating—that is, hyperactivation (Figures 2.1, A and F, and 2.2; see also Supplemental Movie A; all Supplemental Data are available online at www.biolreprod.org). Treatment of fresh, uncapacitated sperm with procaine (Figure 2.1, B and G) or 4-AP (Figure 2.1, C and H) also induced high-amplitude pro-hook beating (see also Supplemental Movies B and C). The maximal response (>90% sperm) was achieved 4 min after adding 5 mM procaine and 1 min after adding 4 mM 4-AP (Figure 2.2). The response triggered by each agent lasted more than 15 min.

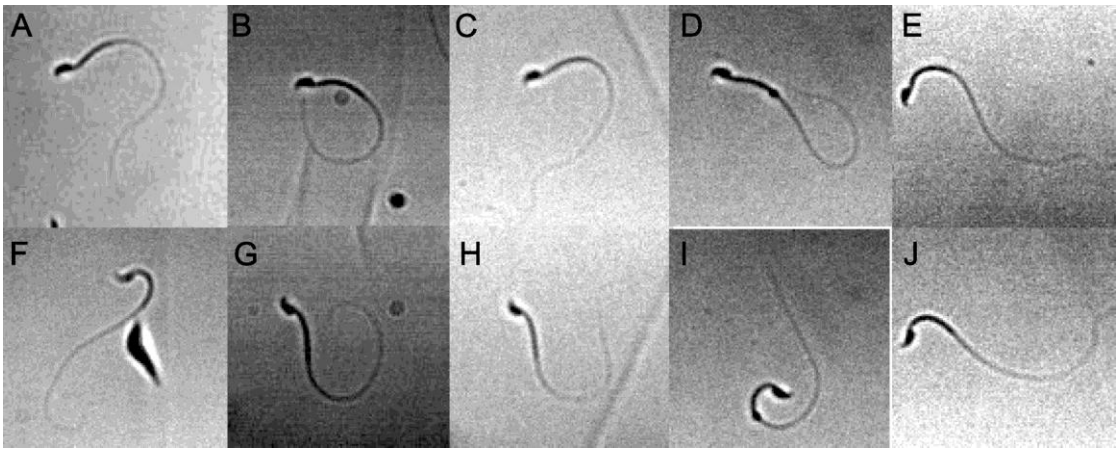

Figure 2.1. Flagellar beating patterns in mouse sperm. Images are individual frames taken from the Supplemental Movies A–E. The upper row of images (**A**–**E**) shows the maximal pro-hook flagellar bends after various treatments, whereas the lower row of images (**F**–**J**) shows the maximal anti-hook flagellar bends. **A** and **F**) Sperm hyperactivated under capacitating conditions. **B** and **G**) Uncapacitated sperm treated with 5 mM procaine. **C** and **H**) Uncapacitated sperm treated with 4 mM 4-AP. **D** and **I**) Uncapacitated sperm treated with 100 μM thimerosal. **E** and **J**) Control (uncapacitated sperm treated with medium).

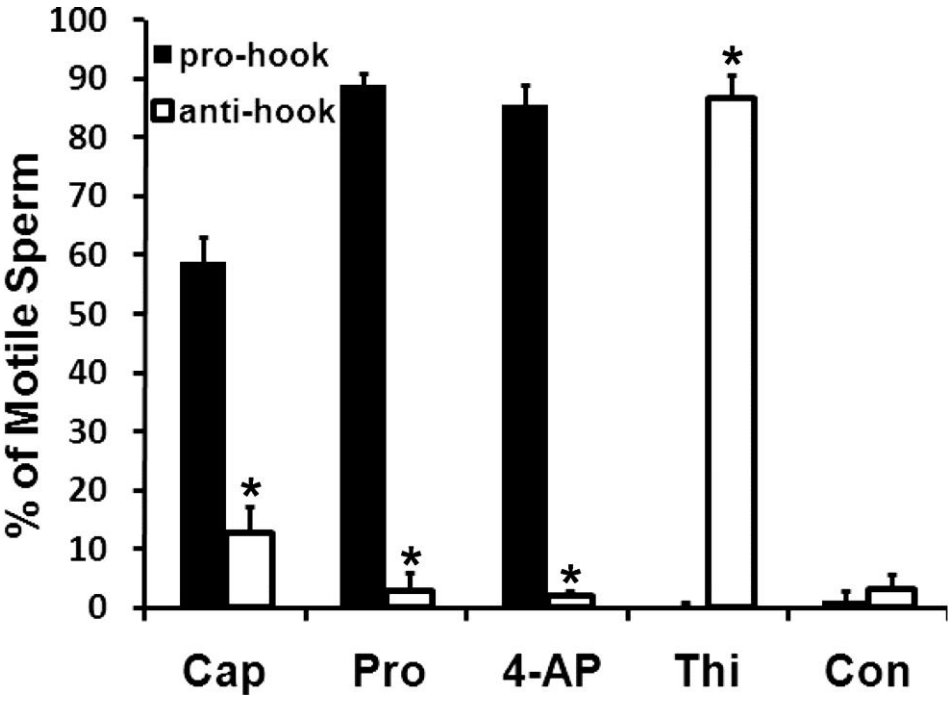

Figure 2.2. Percentage of motile sperm swimming in dominant pro- and anti-hook beating patterns after each treatment. Data are from three males and are presented as

the mean ± SEM. For all treatments, an asterisk (*) indicates a significant difference ($P < 0.01$) between the percentage of dominant pro-hook and anti-hook patterns for each treatment. Cap, capacitated sperm; Pro, 5 mM procaine; 4-AP, 4 mM 4-AP; Thi, 100 μM thimerosal; Con, control sperm.

In contrast to the response to procaine and 4-AP, treatment with 100 μM thimerosal induced high-amplitude anti-hook flagellar beating in 30 sec (Figures 2.1, D and I, and 2.2; see also Supplemental Movie D). The response lasted up to 3 min, and then sperm gradually became sluggish and immotile. Control sperm treated with medium retained nearly symmetrical, low-amplitude flagellar beating, commonly referred to as activated or progressive motility (Figure 2.1, E and J; see also Supplemental Movie E).

Effect of Thimerosal Was Dominant

Thimerosal treatment of sperm that were hyperactivated by incubation under capacitating conditions reversed the direction of the high-amplitude bend in the midpiece region to the anti-hook side of the flagellum. Thimerosal produced a similar reversal in uncapacitated sperm treated with procaine or 4-AP (Figure 2.3A). When uncapacitated sperm were treated first with thimerosal and then with procaine or 4-AP, the dominant beat remained oriented in the anti-hook direction (Figure 2.3B).

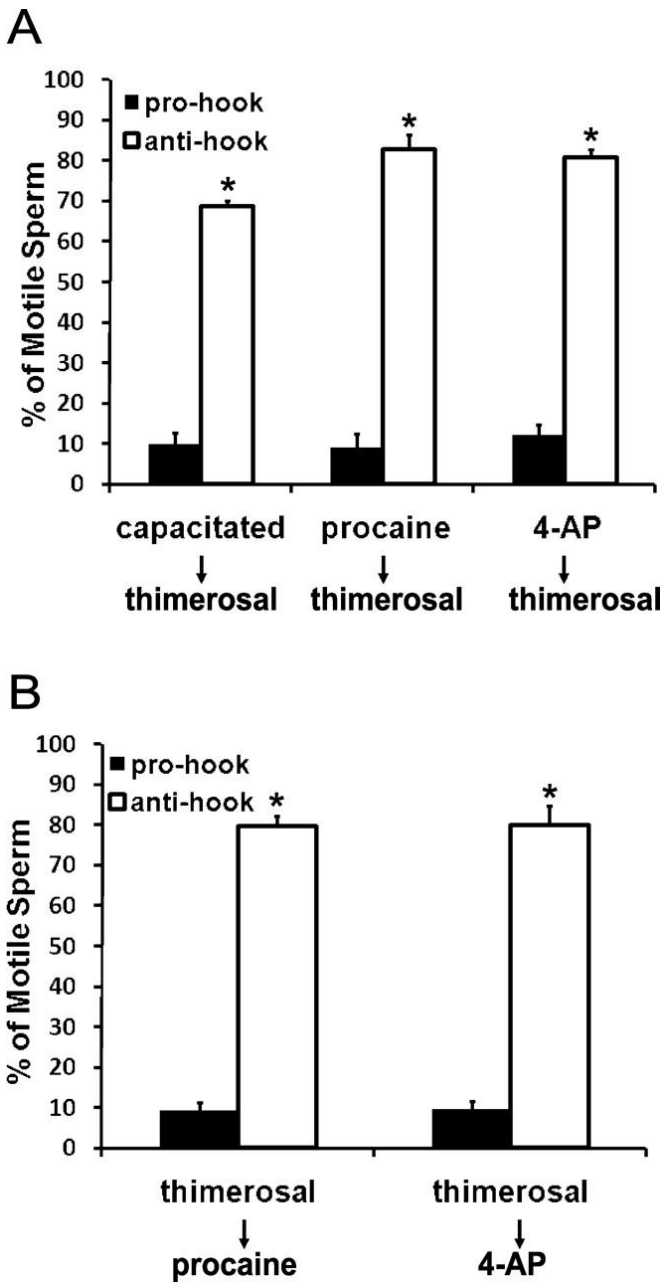

Figure 2.3. Percentage of motile sperm swimming in dominant pro- and anti-hook beating patterns after treatment with a combination of pharmacological agents. **A**) Sperm were treated with 100 μM thimerosal after achieving maximal response to 5 mM procaine or 4 mM 4-AP or after incubation under capacitating conditions for 2 h. **B**) Sperm were treated with 5 mM procaine or 4 mM 4-AP after achieving maximal response by 100 μM thimerosal. Data are from three males and are presented as the mean ± SEM. An asterisk (*) indicates a significant difference ($P < 0.01$) between the percentage of dominant pro-hook and anti-hook patterns for each treatment.

Patterns of Ca^{2+} Increase Differed Between Dominant Pro-Hook and Anti-Hook Beating Patterns

To compare Ca^{2+} increase patterns, sperm were loaded with the fluorescent Ca^{2+} indicator Fluo-4 AM and then adhered to the glass bottom of wells. The fluorescence dynamics were monitored before and after treatments.

After treatment with 4-AP to enhance pro-hook flagellar beating, a Ca^{2+} rise initiated at the midpiece-principal piece junction (Figure 2.4Aa; see also Supplemental Movie F) in 81% (47/58) of sperm and spread to both midpiece and principal piece, whereas during treatment with thimerosal to enhance anti-hook flagellar beating, a Ca^{2+} rise initiated at the base of the flagellum (Figure 2.4 Ac; see also Supplemental Movie H) in 53% (27/51) of sperm. The initiation at the midpiece-principal piece junction was best seen when cytoplasmic droplets were present, because the droplets helped to tether sperm flagellum firmly to the glass bottom of the well. Medium control with 2 mM Ca^{2+} elicited a Ca^{2+}rise in only 4% (2/57) and 5% (3/55) of sperm when no Ca^{2+} was added in the medium (Figure 2.4, Ab and Ad; see also Supplemental Movies G and I). Procaine suppressed the fluorescent signal of the Fluo-4 AM and could not be used for these experiments.

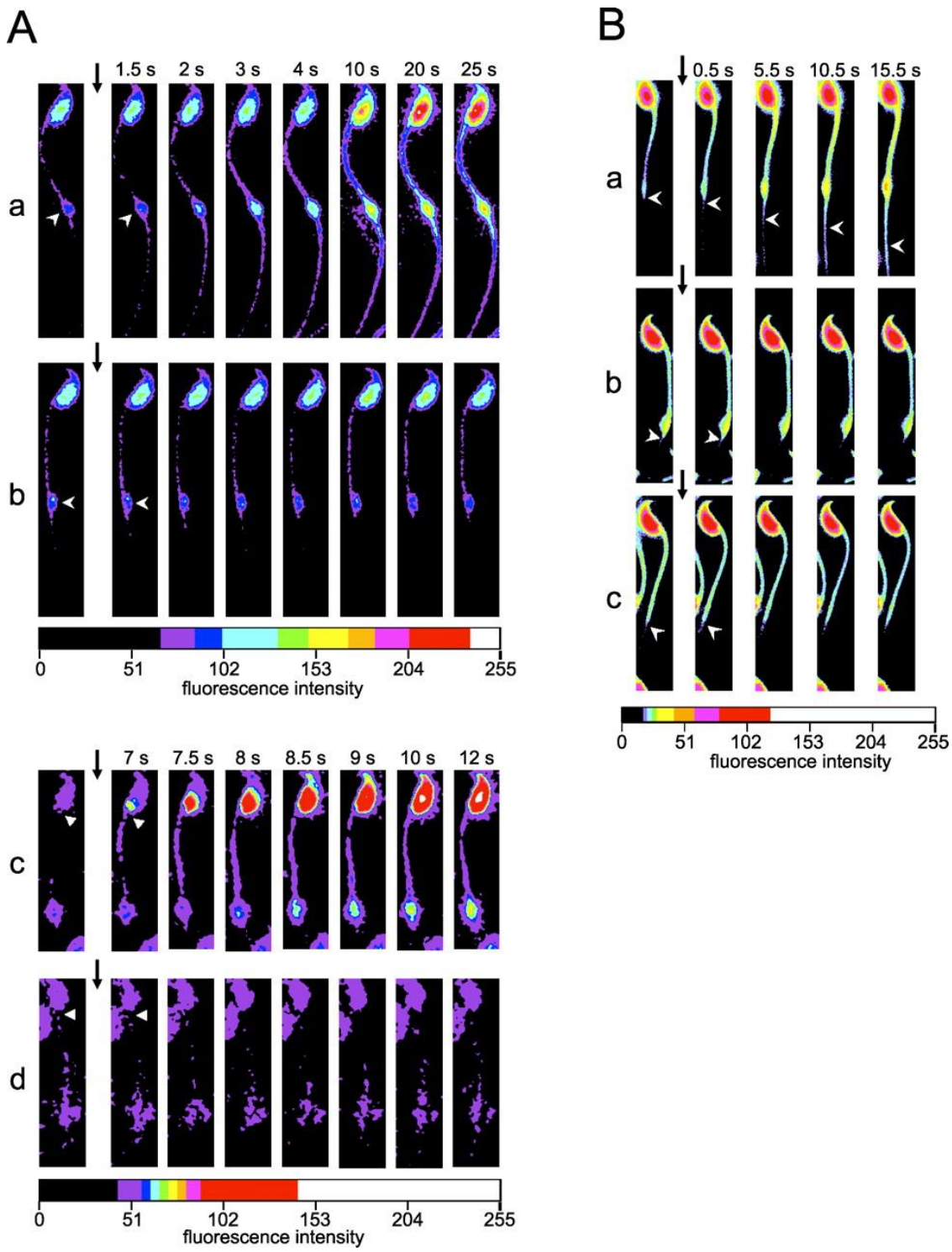

Figure 2.4. **A**) Pseudocolor images of fluorescence of the Ca^{2+} indicator Fluo-4 in sperm treated with 4 mM 4-AP in the presence of 2 mM Ca^{2+} (**a**) or sperm treated with medium as a control (**b**), or with 100 μM thimerosal in the presence of 30 μM Ca^{2+} (**c**) or sperm treated with medium as a control (**d**). Images are colorized individual frames

taken from Supplemental Movies F, G, H, and I, respectively. Elapsed time is indicated above the images, and arrows indicate time of addition. The base of the flagellum is indicated by triangles, and the cytoplasmic droplet is indicated by arrowheads. Warmer colors indicate higher Ca^{2+}. **B**) Pseudocolor images of fluorescence of pH indicator BCECF in sperm treated with 4 mM 4-AP (**a**), 100 μM thimerosal (**b**), or medium control (**c**). Images are colorized individual frames taken from Supplemental Movies J, K, and L, respectively. Elapsed time is indicated above the images, and arrows indicate time of addition. In **a**, the arrowheads indicate the increased signal in the principal piece; in **b** and **c**, the arrowheads indicate the proximal principal piece. Warmer colors indicate higher pH.

During Enhancement of Pro-Hook Bending by 4-AP, Rise in Flagellar pH Accompanied Ca^{2+} Rise

To investigate whether pH change was involved in increasing either pro- or anti-hook flagellar bends, sperm were loaded with the fluorescent pH indicator BCECF-AM to monitor pH change before and after various treatments. Imaging of individual sperm revealed that 4-AP application produced a pH rise in the principal piece of the flagellum within 1 sec in 85% (47/55) of sperm examined (Figure 2.4 Ba; see also Supplemental Movie J). Neither thimerosal nor medium control triggered a detectable pH change (Figure 2.4, Bb and Bc; see also Supplemental Movies K and L). When the fluorescence of populations of sperm in multiwell plates was monitored, only 4-AP triggered a steady increase in fluorescence (Figure 2.5).

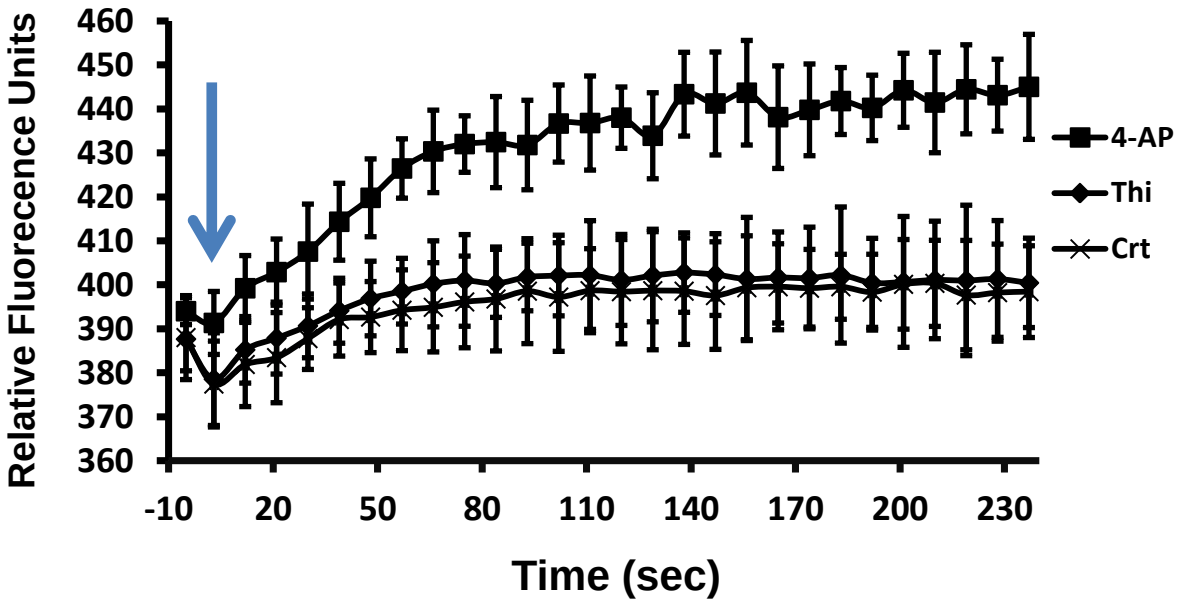

Figure 2.5. The fluorescence of the pH indicator BCECF in sperm populations monitored using a microplate reader. Arrow indicates time of addition. Data are from three males and are presented as the mean ± SEM.

As was the case with our attempts at detecting fluorescence of the Ca^{2+} indicator, we were unable to test the effect of procaine on pH dynamics, because procaine interfered with the fluorescent signals, which was verified using the Bio-Tek plate reader (data not shown).

Pharmacological Treatments Did Not Induce Acrosome Reactions

Increases of Ca^{2+} in the head can induce acrosome reactions, which could complicate analysis. The Coomassie blue staining showed that none of the pharmacological treatments, which were performed on uncapacitated sperm, induced

acrosome reactions except for the positive-control treatment with the Ca^{2+} ionophore A23187 (Figure 2.6).

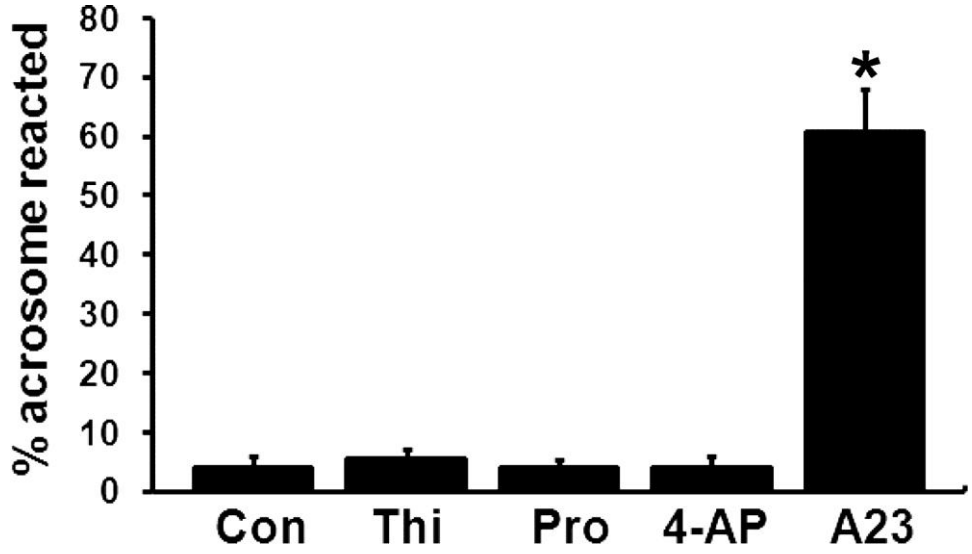

Figure 2.6. Percentage of acrosome-reacted sperm in response to treatments with procaine, 4-AP, thimerosal, and medium control. The positive control is A23187, a Ca^{2+} ionophore. Data are from three males and are presented as the mean ± SEM. An asterisk (*) indicates a significant difference ($P < 0.01$) from the medium (negative) control. Con, control sperm; Thi, 100 μM thimerosal; Pro, 5 mM procaine; A23, 20 μM A23187; 4-AP, 4 mM 4-AP.

Treatment by Pharmacological Agents Did Not Phosphorylate Proteins on Tyrosine

One-dimensional SDS-PAGE electrophoresis followed by Western blot using antiphosphotyrosine antibody revealed that neither procaine, 4-AP, nor thimerosal stimulated detectable increases in tyrosine phosphorylation, despite producing motility responses in nearly 90% of the sperm. Only incubation of sperm under capacitating conditions promoted tyrosine phosphorylation (Figure 2.7).

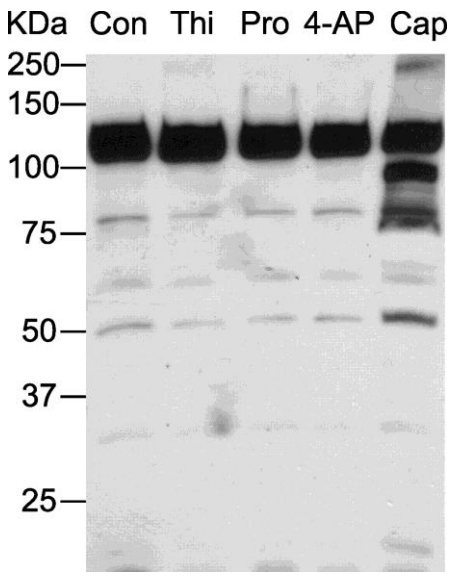

Figure 2.7. One-dimensional electrophoresis followed by Western blot detection of proteins phosphorylated on tyrosine after various treatments. Con, control sperm; Thi, 100 μM thimerosal; Pro, 5 mM procaine; 4-AP, 4 mM 4-AP; Cap, capacitated sperm.

Enhancement of Pro- and Anti-Hook Flagellar Bending Produced Different Threonine and Serine Phosphorylation Patterns

Treatment with procaine, 4-AP, or thimerosal resulted in the phosphorylation of so many proteins on threonine and serine that two-dimensional electrophoresis and Western blot analysis were required to distinguish phosphorylation patterns. Incubation under capacitating conditions or treatment with procaine or 4-AP produced phosphorylation of several proteins on threonine and serine relative to the control (Figure 2.8), in particular proteins of approximately 75 kDa and pH 4–6 and proteins of 25–30 kDa and pH 4.5–9.3 (Figure 2.8, A–C). Differences were seen in phosphorylation patterns among sperm treated by capacitation, procaine, and 4-AP.

For example, capacitation produced more phosphorylation than the other two treatments in proteins with a mass of approximately 60 kDa and pH 6.0–9.3 (Figure 2.8 A). Also, the blots from sperm treated with procaine did not show phosphoserine-containing proteins at 50–75 kDa and pH 5.8–6.5. Enhancement of anti-hook bending by thimerosal dephosphorylated some proteins, such as those of approximately 60 kDa and pH 4–4.5 (Figure 2.8 D).

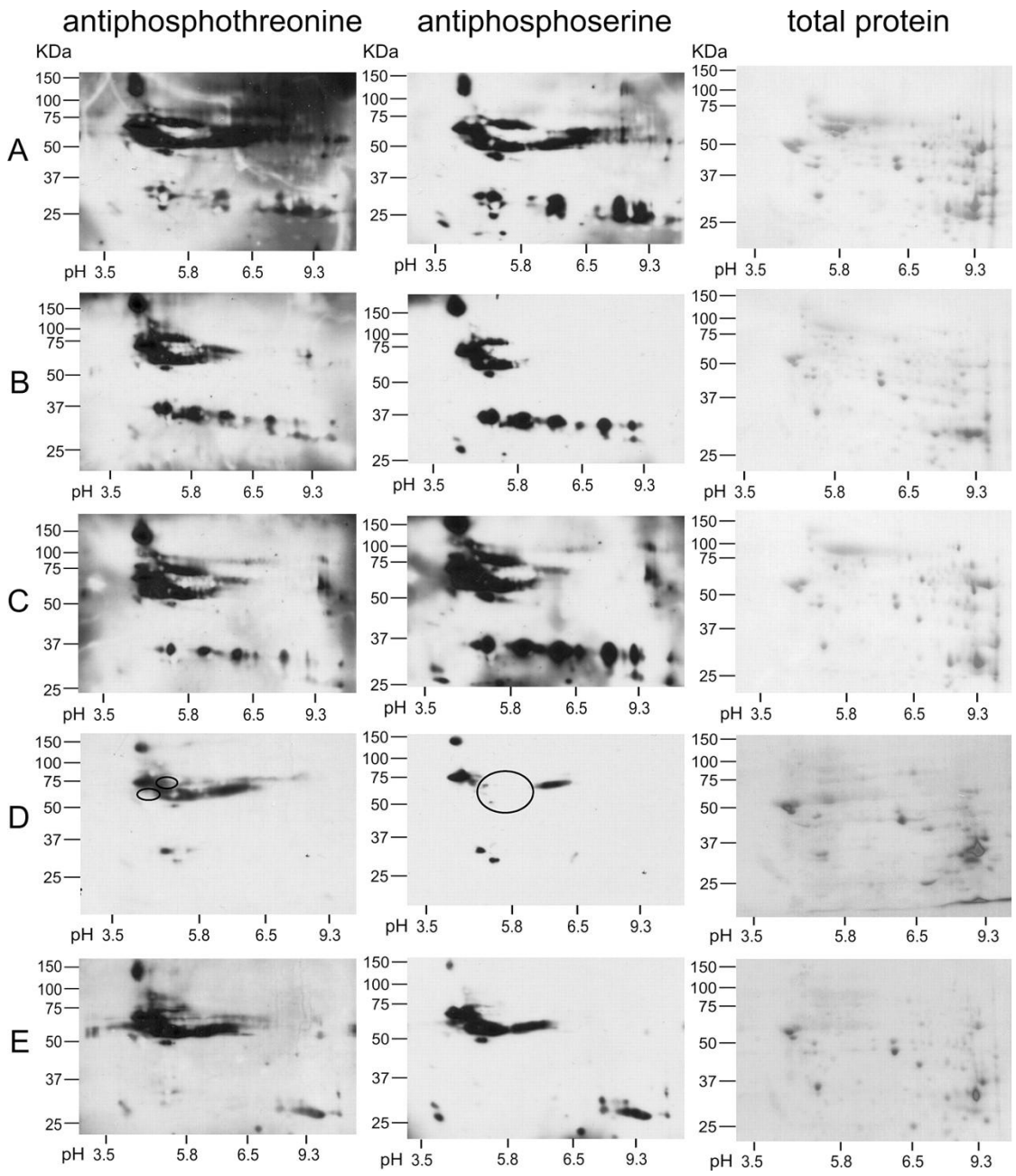

Figure 2.8. Two-dimensional electrophoresis followed by Western blot detection of proteins phosphorylated on serine and threonine after various treatments. **A)** Capacitated sperm. **B)** 5 mM procaine. **C)** 4 mM 4-AP. **D)** 100 μM thimerosal (circles indicate major reductions in phosphorylation compared with E). **E)** Control sperm.

Immunocytochemistry was used to locate the threonine- or serine-phosphorylated proteins involved in dominant pro- and anti-hook bending. Antiphosphothreonine and antiphosphoserine antibody labeling showed that procaine and 4-AP generally increased phosphorylation (Figure 2.9, A and B), whereas thimerosal decreased phosphorylation (Figure 2.9 C). Serine phosphorylation by procaine and 4-AP was concentrated at the base of the flagellum, whereas threonine phosphorylation was concentrated in the head and principal piece of the flagellum (Figure 2.9, A and B).

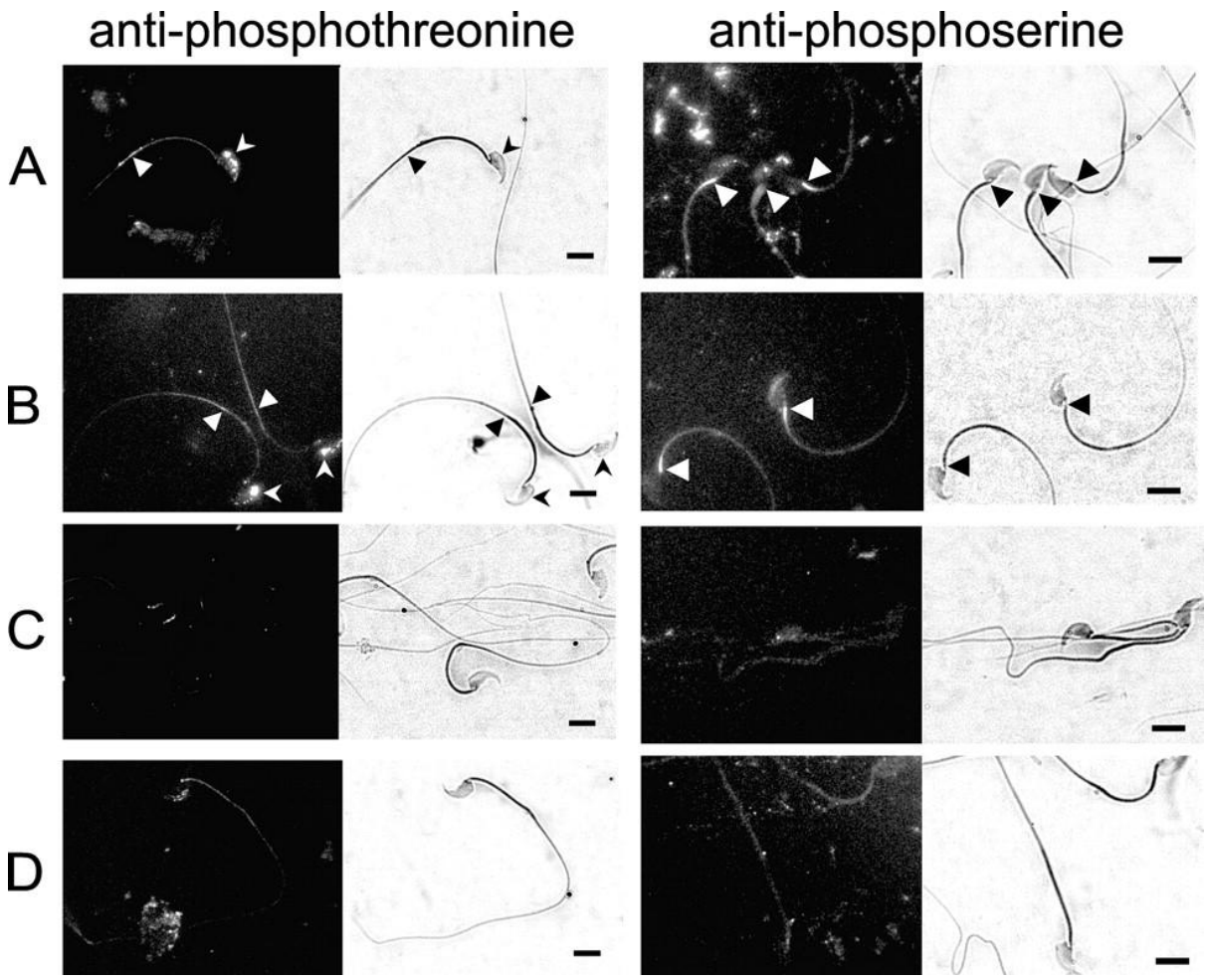

Figure 2.9. Immunofluorescent localization of proteins phosphorylated on serine and threonine after various treatments. Immunofluorescence images are shown on the left and corresponding bright-field images on the right. For phosphothreonine images, the principal piece of sperm is indicated by triangles, and the head is indicated by arrowheads. For phosphoserine images, the base of the flagellum is indicated by triangles. **A)** 5 mM Procaine. **B)** 4 mM 4-AP. **C)** 100 μM thimerosal. **D)** Medium control. Bar = 10 μm.

DISCUSSION

In the present study, we characterized the dynamics of Ca^{2+}, pH, and protein phosphorylation patterns associated with dominant pro- and anti-hook flagellar

bending in mouse sperm. Because capacitation [27, 28], procaine [22, 24], and 4-AP [25] have been shown to activate CATSPER channels, our data indicate that activation of CATSPER channels produces dominant pro-hook beating. In contrast, stimulation of Ca^{2+} release from stores by thimerosal produced dominant anti-hook beating. Only dominant pro-hook beating was accompanied by a rise in pH and was associated with increased serine/threonine phosphorylation, whereas dominant anti-hook beating was associated with dephosphorylation of some proteins. Tyrosine phosphorylation was unaffected by any of the pharmacological agents. Altogether, our results demonstrate that two distinct Ca^{2+} signaling pathways induce these two types of asymmetrical beating.

Although the asymmetry of the flagellar bending is integral to the definition of hyperactivation, little attention has been given to characterizing this asymmetry with reference to the orientation of sperm heads. This is because the sperm heads of many species, including humans and cattle, are symmetrical, making it impossible to discern the direction of the bend. By using the asymmetrical hook on the head of mouse sperm as a reference for the direction of the flagellar bend, we were able to identify two distinct kinds of asymmetrical beating. Procaine [24, 29–32], 4-AP [33, 34], and thimerosal [21] are reported to trigger hyperactivation in the sperm of humans, guinea pigs, and cattle, but the response to thimerosal might actually be the reverse of the response to procaine and 4-AP.

In our experiments, 4-AP increased Ca^{2+} and pH in the principal piece, indicating the activation of CATSPER channels. We found that this 4-AP-triggered

Ca^{2+} rise began at the midpiece-principal piece junction of the flagellum of sperm and spread not only distally to the principal piece, where CATSPER channels are located [12, 13], but also proximally to the midpiece and head (Figure 2.4 A). This observation is similar to that reported by Xia *et al.* [35], who observed that the Ca^{2+} entry mediated by CATSPER channels starts at the principal piece before propagating to the head. It has been reported that 4-AP enhances the CATSPER channel current [25], and it has been suggested that 4-AP induces intracellular alkalinization [36]. In sperm, alkalinization activates CATSPER channels [13, 25, 27, 28, 35, 37, 38] (for review, see [14]). Our results show that only 4-AP triggered a pH increase in the principal piece of the flagellum. The pH increase in the principal piece upon 4-AP treatment occurred within 1 sec (Figure 2.4 Ba), which was before the initiation of the Ca^{2+} increase (Figure 2.4 Aa). This is consistent with previous findings that intracellular alkalization occurs before increase of Ca^{2+} in hyperactivated bovine sperm [39]. Thus, we conclude that 4-AP indirectly activates CATSPER channels to produce pro-hook bending.

Thimerosal triggers asymmetrical beating by releasing Ca^{2+} from the RNE store. In our experiments with mouse sperm, thimerosal triggered a Ca^{2+} release at the neck of the flagellum that spread into the postacrosomal region of the head and the midpiece. Thimerosal has been found to trigger Ca^{2+} release from both IP_3- and ryanodine-sensitive calcium stores in many cell types (for review, see [40]). The presence of RNE at the base of the flagellum has been observed in mature sperm of several species [41–44]. In bovine sperm, labeling with antibody to IP_3 receptor

demonstrated the presence of the receptor in the RNE stores. Also, treatment with thimerosal and thapsigargin, even in the absence of available extracellular Ca^{2+}, triggered asymmetrical flagellar beating in bull sperm [21].

Despite inducing a rise in Ca^{2+} in the sperm head, neither 4-AP, procaine, nor thimerosal treatments elicited acrosome reactions in these uncapacitated sperm, which would have confounded interpretation of the effects of these agents on flagellar beating patterns. In other work, procaine and thimerosal also did not induce acrosome reactions in equine sperm [32] and in bull sperm [21].

In many types of cells, Ca^{2+} signaling is often accompanied by protein phosphorylation [45]. Our results show that procaine and 4-AP triggered phosphorylation on serine and threonine sites of several proteins, whereas thimerosal treatment dephosphorylated some proteins. Serine phosphorylation induced by procaine and 4-AP was generally located in the head and the entire flagellum but most prominently at the base, whereas threonine phosphorylated proteins were most prominent in the head and principal piece of the flagellum. In all labeled regions, increased Ca^{2+} was detected in response to 4-AP. In contrast to 4-AP, thimerosal generally reduced phosphorylation, suggesting that the downstream proteins of Ca^{2+} mobilization were quite different from those involved in pro-hook bending triggered by 4-AP. We concluded that the Ca^{2+} signaling pathways were different for dominant pro- and anti-hook bending, which might be referred to as hyperactivation and reverse hyperactivation.

Different patterns of protein phosphorylation/dephosphorylation could occur if the initial targets of the increased Ca^{2+} were different during amplification of pro-hook and anti-hook bending. Calmodulin is known to play a role in Ca^{2+}-dependent modulation of mammalian sperm flagellar beating by directly affecting the axoneme [46]. Evidence indicates additional Ca^{2+}-binding proteins in sperm flagella, such as CABYR in mammals [47, 48] and calaxin, in the ascidian *Ciona intestinalis* [49]. Also, in *Chlamydomonas* sp., the dynein light chain protein LC4 has been localized in the flagella and shown to undergo a conformation change in response to Ca^{2+} [50]. Calaxin and LC4, as well as additional Ca^{2+}-binding axonemal proteins, may yet be identified in mammalian sperm. The downstream targets of these proteins would likely differ from those of calmodulin. Also, it would be expected that the different Ca^{2+}-binding proteins responsible for amplifying pro-hook and anti-hook flagellar beating would show different ultrastructural distributions in the axoneme, particularly with respect to the side of the axoneme on which they are located.

To our knowledge, the present publication is the first report of the occurrence of serine/threonine phosphorylation during mouse sperm hyperactivation. Serine and threonine phosphorylation in general is not well understood because of a historical lack of antibodies with high specificity. To date, most serine/threonine phosphorylation studies in sperm have focused on activation, capacitation, and the acrosome reaction. In those studies, both phosphorylation and dephosphorylation have been implicated in those processes [51–55]. Several kinases [46, 56–58] and

phosphatases [59–63] have been implicated in the regulation of sperm motility patterns.

Tyrosine phosphorylation on a series of proteins is an established hallmark of capacitation [64]. Hyperactivation is generally considered to be a part of capacitation. However, hyperactivation has been observed to occur independently of other aspects of capacitation [31]. Neither 4-AP, procaine, nor thimerosal induced detectable tyrosine phosphorylation in our experiments; instead, the tyrosine phosphorylation was affected only by capacitating conditions. It was reported that procaine does not affect tyrosine phosphorylation in bovine and equine sperm [31, 32]. This means proteins that are tyrosine phosphorylated during capacitation do not play a direct role in hyperactivation downstream of the action of procaine, 4-AP, or thimerosal, although tyrosine phosphorylation may operate upstream of the effects of these agents in the activation of Ca^{2+} influx or release from stores.

In our experiments, we found it was possible to reverse capacitation-associated hyperactivation or agent-amplified pro-hook beating using thimerosal, indicating that the effect of thimerosal is dominant. Thimerosal (100 μM) arrested sperm in approximately 3 min. The arrest of motility could be the result of deleterious effects of prolonged elevation of cytosolic Ca^{2+}.

In other cell types, release of Ca^{2+} from stores briefly produces micromolar levels of Ca^{2+} in the immediate vicinity of the store [45, 65]. In vivo, the short burst of Ca^{2+} from the RNE triggered by physiological factor(s) could induce a brief reversal

of the dominant flagellar bend from pro- to anti-hook, and then Ca^{2+} could be rapidly removed by the mitochondria near the RNE and also pumped back into the RNE stores or out through the plasma membrane by Ca^{2+} ATPases [65, 66]. The momentary large anti-hook bend could produce a course correction in sperm, perhaps reorienting them toward the oocyte.

Sperm hyperactivated during capacitation exhibited a small anti-hook bend very close to the head during the reverse phase of the beat, similar to that seen in activated sperm. Surprisingly, this small anti-hook bend was not seen in sperm hyperactivated by procaine or 4-AP (Figure 2.1; see also Supplemental Movies A–C). Carlson et al. [24] also reported that capacitated sperm showed different midpiece curvature in the pro- and anti-hook directions than procaine-treated sperm. The small anti-hook bend could result from a small release of Ca^{2+} from stores that is not triggered by procaine or 4-AP or other ionic or molecular differences in the cytoplasm at the base of the flagellum.

In a variety of marine invertebrate species, including the sea urchin *Arbacia punctulata*, sperm respond to chemotactic signals from the oocytes through Ca^{2+}-mediated changes in flagellar beat asymmetry (for review, see [67]). Specifically, the flagellar beating patterns alternate between asymmetrical and nearly symmetrical patterns, resulting in a swimming trajectory that alternates between high and low curvature. This alternation forms a "turn and run" pattern, which produces a loosely helical configuration with an axis that is directed toward the source of the attractant (for review, see [68]). Some evidence exists for sperm chemotaxis in mammals as well

(for review, see [23]). Nevertheless, the details of the flagellar response of mammalian sperm to chemoattractants are not well elucidated and may be different from those of invertebrate sperm. In mammals, chemoattractant(s) from the oocytes could modulate the flagellar beating of hyperactivated sperm by releasing Ca^{2+} from the RNE store. This is supported by our observation that thimerosal could reverse the bend pattern of sperm that were hyperactivated by incubation under capacitating conditions.

We have proposed that hyperactivated sperm require intermittent course corrections to reach the oocyte, because sperm begin to hyperactivate in the oviduct far from the site of fertilization [4]. We have now provided evidence for a mechanism to make course corrections. Here, we have shown that the dominant bend of hyperactivated sperm can be switched to the anti-hook direction by release of Ca^{2+} from intracellular Ca^{2+} stores via a signal transduction pathway that is distinct from the Ca^{2+} pathway that triggers hyperactivation through activation of CATSPER channels. Much remains to be learned about the how hyperactivation is modulated to bring sperm to the oocyte. Hopefully, the clues offered by the hook-shaped heads of rodent sperm will continue to offer insight regarding these mechanisms.

ACKNOWLEDGMENT

The authors would like to acknowledge Dr. Becky Marquez for first bringing the anti-hook swimming pattern of sperm to our attention when she was a graduate student in our laboratory.

REFERENCES

1. Yanagimachi R. The movement of golden hamster spermatozoa before and after capacitation. J Reprod Fertil 1970; 23:193-196.

2. Visconti PE. Understanding the molecular basis of sperm capacitation through kinase design. Proc Natl Acad Sci U S A 2009; 106:667-668.

3. Suarez SS, Pacey AA. Sperm transport in the female reproductive tract. Hum Reprod Update 2006; 12:23-37.

4. Suarez SS, Osman RA. Initiation of hyperactivated flagellar bending in mouse sperm within the female reproductive tract. Biol Reprod 1987; 36:1191-1198.

5. DeMott RP, Suarez SS. Hyperactivated sperm progress in the mouse oviduct. Biol Reprod 1992; 46:779-785.

6. Pacey AA, Davies N, Warren MA, Barratt CL, Cooke ID. Hyperactivation may assist human spermatozoa to detach from intimate association with the endosalpinx. Hum Reprod 1995; 10:2603-2609.

7. Ho K, Wolff CA, Suarez SS. CatSper-null mutant spermatozoa are unable to ascend beyond the oviductal reservoir. Reprod Fertil Dev 2009; 21:345-350.

8. Suarez SS, Katz DF, Owen DH, Andrew JB, Powell RL. Evidence for the function of hyperactivated motility in sperm. Biol Reprod 1991; 44:375-381.

9. Suarez SS, Dai XB, DeMott RP, Redfern K, Mirando MA. Movement characteristics of boar sperm obtained from the oviduct or hyperactivated in vitro. J Androl 1992; 13:75-80.

10. Quill TA, Sugden SA, Rossi KL, Doolittle LK, Hammer RE, Garbers DL. Hyperactivated sperm motility driven by CatSper2 is required for fertilization. Proc Natl Acad Sci U S A 2003; 100:14869-14874.

11. Stauss CR, Votta TJ, Suarez SS. Sperm motility hyperactivation facilitates penetration of the hamster zona pellucida. Biol Reprod 1995; 53:1280-1285.

12. Ren D, Navarro B, Perez G, Jackson AC, Hsu S, Shi Q, Tilly JL, Clapham DE. A sperm ion channel required for sperm motility and male fertility. Nature 2001; 413:603-609.

13. Quill TA, Ren D, Clapham DE, Garbers DL. A voltage-gated ion channel expressed specifically in spermatozoa. Proc Natl Acad Sci U S A 2001; 98:12527-12531.

14. Navarro B, Kirichok Y, Chung JJ, Clapham DE. Ion channels that control fertility in mammalian spermatozoa. Int J Dev Biol 2008; 52:607-613.

15. Publicover SJ, Giojalas LC, Teves ME, de Oliveira GS, Garcia AA, Barratt CL, Harper CV. Ca2+ signalling in the control of motility and guidance in mammalian sperm. Front Biosci 2008; 13:5623-5637.

16. Suarez SS. Control of hyperactivation in sperm. Hum Reprod Update 2008; 14:647-657.

17. Overstreet JW, Cooper GW. Effect of ovulation and sperm motility on the migration of rabbit spermatozoa to the site of fertilization. J Reprod Fertil 1979; 55:53-59.

18. Carlson AE, Burnett LA, del Camino D, Quill TA, Hille B, Chong JA, Moran MM, Babcock DF. Pharmacological targeting of native CatSper channels reveals a required role in maintenance of sperm hyperactivation. PLoS One 2009; 4:e6844.

19. Bootman MD, Taylor CW, Berridge MJ. The thiol reagent, thimerosal, evokes Ca2+ spikes in HeLa cells by sensitizing the inositol 1,4,5-trisphosphate receptor. J Biol Chem 1992; 267:25113-25119.

20. Lytton J, Westlin M, Hanley MR. Thapsigargin inhibits the sarcoplasmic or endoplasmic reticulum Ca-ATPase family of calcium pumps. J Biol Chem 1991; 266:17067-17071.

21. Ho HC, Suarez SS. An inositol 1,4,5-trisphosphate receptor-gated intracellular Ca(2+) store is involved in regulating sperm hyperactivated motility. Biol Reprod 2001; 65:1606-1615.

22. Marquez B, Ignotz G, Suarez SS. Contributions of extracellular and intracellular Ca2+ to regulation of sperm motility: Release of intracellular stores can hyperactivate CatSper1 and CatSper2 null sperm. Dev Biol 2007; 303:214-221.

23. Chang H, Suarez SS. Rethinking the Relationship Between Hyperactivation and Chemotaxis in Mammalian Sperm. Biol Reprod 2010; 83:507-513.

24. Carlson AE, Quill TA, Westenbroek RE, Schuh SM, Hille B, Babcock DF. Identical phenotypes of CatSper1 and CatSper2 null sperm. J Biol Chem 2005; 280:32238-32244.

25. Navarro B, Kirichok Y, Clapham DE. KSper, a pH-sensitive K+ current that controls sperm membrane potential. Proc Natl Acad Sci U S A 2007; 104:7688-7692.

26. Miller DJ, Gong X, Shur BD. Sperm require beta-N-acetylglucosaminidase to penetrate through the egg zona pellucida. Development 1993; 118:1279-1289.

27. Kirichok Y, Navarro B, Clapham DE. Whole-cell patch-clamp measurements of spermatozoa reveal an alkaline-activated Ca2+ channel. Nature 2006; 439:737-740.

28. Qi H, Moran MM, Navarro B, Chong JA, Krapivinsky G, Krapivinsky L, Kirichok Y, Ramsey IS, Quill TA, Clapham DE. All four CatSper ion channel proteins are required for male fertility and sperm cell hyperactivated motility. Proc Natl Acad Sci U S A 2007; 104:1219-1223.

29. Lindemann CB, Goltz JS, Kanous KS, Gardner TK, Olds-Clarke P. Evidence for an increased sensitivity to Ca2+ in the flagella of sperm from tw32/+mice. Mol Reprod Dev 1990; 26:69-77.

30. Mujica A, Neri-Bazan L, Tash JS, Uribe S. Mechanism for procaine-mediated hyperactivated motility in guinea pig spermatozoa. Mol Reprod Dev 1994; 38:285-292.

31. Marquez B, Suarez SS. Different signaling pathways in bovine sperm regulate capacitation and hyperactivation. Biol Reprod 2004; 70:1626-1633.

32. McPartlin LA, Suarez SS, Czaya CA, Hinrichs K, Bedford-Guaus SJ. Hyperactivation of stallion sperm is required for successful in vitro fertilization of equine oocytes. Biol Reprod 2009; 81:199-206.

33. Gu Y, Kirkman-Brown JC, Korchev Y, Barratt CL, Publicover SJ. Multi-state, 4-aminopyridine-sensitive ion channels in human spermatozoa. Dev Biol 2004; 274:308-317.

34. Bedu-Addo K, Costello S, Harper C, Machado-Oliveira G, Lefievre L, Ford C, Barratt C, Publicover S. Mobilisation of stored calcium in the neck region of human sperm--a mechanism for regulation of flagellar activity. Int J Dev Biol 2008; 52:615-626.

35. Xia J, Reigada D, Mitchell CH, Ren D. CATSPER channel-mediated Ca2+ entry into mouse sperm triggers a tail-to-head propagation. Biol Reprod 2007; 77:551-559.

36. Howe JR, Ritchie JM. On the active form of 4-aminopyridine: block of K+ currents in rabbit Schwann cells. J Physiol 1991; 433:183-205.

37. Carlson AE, Westenbroek RE, Quill T, Ren D, Clapham DE, Hille B, Garbers DL, Babcock DF. CatSper1 required for evoked Ca2+ entry and control of flagellar function in sperm. Proc Natl Acad Sci U S A 2003; 100:14864-14868.

38. Lishko PV, Botchkina IL, Fedorenko A, Kirichok Y. Acid extrusion from human spermatozoa is mediated by flagellar voltage-gated proton channel. Cell; 140:327-337.

39. Marquez B, Suarez SS. Bovine sperm hyperactivation is promoted by alkaline-stimulated Ca2+ influx. Biol Reprod 2007; 76:660-665.

40. Elferink JG. Thimerosal: a versatile sulfhydryl reagent, calcium mobilizer, and cell function-modulating agent. Gen Pharmacol 1999; 33:1-6.

41. Franklin LE. Formation of the redundant nuclear envelope in monkey spermatids. Anat Rec 1968; 161:149-161.

42. Ho HC, Suarez SS. Characterization of the intracellular calcium store at the base of the sperm flagellum that regulates hyperactivated motility. Biol Reprod 2003; 68:1590-1596.

43. Rouse GW, Robson SK. An ultrastructural study of megachiropteran (Mammalia: Chiroptera) spermatozoa: implications for chiropteran phylogeny. J Submicrosc Cytol 1986; 18:137-152.

44. Toshimori K, Higashi R, Oura C. Distribution of intramembranous particles and filipin-sterol complexes in mouse sperm membranes: polyene antibiotic filipin treatment. Am J Anat 1985; 174:455-470.

45. Clapham DE. Calcium signaling. Cell 2007; 131:1047-1058.

46. Ignotz GG, Suarez SS. Calcium/calmodulin and calmodulin kinase II stimulate hyperactivation in demembranated bovine sperm. Biol Reprod 2005; 73:519-526.

47. Naaby-Hansen S, Mandal A, Wolkowicz MJ, Sen B, Westbrook VA, Shetty J, Coonrod SA, Klotz KL, Kim YH, Bush LA, Flickinger CJ, Herr JC. CABYR,

a novel calcium-binding tyrosine phosphorylation-regulated fibrous sheath protein involved in capacitation. Dev Biol 2002; 242:236-254.

48. Newell AE, Fiedler SE, Ruan JM, Pan J, Wang PJ, Deininger J, Corless CL, Carr DW. Protein kinase A RII-like (R2D2) proteins exhibit differential localization and AKAP interaction. Cell Motil Cytoskeleton 2008; 65:539-552.

49. Mizuno K, Padma P, Konno A, Satouh Y, Ogawa K, Inaba K. A novel neuronal calcium sensor family protein, calaxin, is a potential Ca(2+)-dependent regulator for the outer arm dynein of metazoan cilia and flagella. Biol Cell 2009; 101:91-103.

50. Sakato M, Sakakibara H, King SM. Chlamydomonas outer arm dynein alters conformation in response to Ca2+. Mol Biol Cell 2007; 18:3620-3634.

51. Naz RK. Involvement of protein serine and threonine phosphorylation in human sperm capacitation. Biol Reprod 1999; 60:1402-1409.

52. Jha KN, Shivaji S. Protein serine and threonine phosphorylation, hyperactivation and acrosome reaction in in vitro capacitated hamster spermatozoa. Mol Reprod Dev 2002; 63:119-130.

53. Krapf D, Arcelay E, Wertheimer EV, Sanjay A, Pilder SH, Salicioni AM, Visconti PE. Inhibition of Ser/Thr phosphatases induces capacitation-associated signaling in the presence of Src kinase inhibitors. J Biol Chem; 285:7977-7985.

54. kJha KN, Salicioni AM, Arcelay E, Chertihin O, Kumari S, Herr JC, Visconti PE. Evidence for the involvement of proline-directed serine/threonine phosphorylation in sperm capacitation. Mol Hum Reprod 2006; 12:781-789.

55. Alnagar FA, Brennan P, I AB. Bicarbonate-dependent serine/threonine protein dephosphorylation in capacitating boar spermatozoa. J Androl; 31:393-405.

56. Schlingmann K, Michaut MA, McElwee JL, Wolff CA, Travis AJ, Turner RM. Calmodulin and CaMKII in the sperm principal piece: evidence for a motility-related calcium/calmodulin pathway. J Androl 2007; 28:706-716.

57. Marin-Briggiler CI, Jha KN, Chertihin O, Buffone MG, Herr JC, Vazquez-Levin MH, Visconti PE. Evidence of the presence of calcium/calmodulin-dependent protein kinase IV in human sperm and its involvement in motility regulation. J Cell Sci 2005; 118:2013-2022.

58. Visconti PE, Moore GD, Bailey JL, Leclerc P, Connors SA, Pan D, Olds-Clarke P, Kopf GS. Capacitation of mouse spermatozoa. II. Protein tyrosine

phosphorylation and capacitation are regulated by a cAMP-dependent pathway. Development 1995; 121:1139-1150.

59. Tash JS, Bracho GE. Regulation of sperm motility: emerging evidence for a major role for protein phosphatases. J Androl 1994;15: 505-509.

60. Tash JS, Krinks M, Patel J, Means RL, Klee CB, Means AR. Identification, characterization, and functional correlation of calmodulin-dependent protein phosphatase in sperm. J Cell Biol 1988; 106:1625-1633.

61. Puri P, Myers K, Kline D, Vijayaraghavan S. Proteomic analysis of bovine sperm YWHA binding partners identify proteins involved in signaling and metabolism. Biol Reprod 2008; 79:1183-1191.

62. Smith GD, Wolf DP, Trautman KC, da Cruz e Silva EF, Greengard P, Vijayaraghavan S. Primate sperm contain protein phosphatase 1, a biochemical mediator of motility. Biol Reprod 1996; 54:719-727.

63. Vijayaraghavan S, Stephens DT, Trautman K, Smith GD, Khatra B, da Cruz e Silva EF, Greengard P. Sperm motility development in the epididymis is associated with decreased glycogen synthase kinase-3 and protein phosphatase 1 activity. Biol Reprod 1996; 54:709-718.

64. Visconti PE, Bailey JL, Moore GD, Pan D, Olds-Clarke P, Kopf GS. Capacitation of mouse spermatozoa. I. Correlation between the capacitation state and protein tyrosine phosphorylation. Development 1995; 121:1129-1137.

65. Berridge MJ. Calcium microdomains: organization and function. Cell Calcium 2006; 40:405-412.

66. Wennemuth G, Babcock DF, Hille B. Calcium clearance mechanisms of mouse sperm. J Gen Physiol 2003; 122:115-128.

67. Kaupp UB, Hildebrand E, Weyand I. Sperm chemotaxis in marine invertebrates--molecules and mechanisms. J Cell Physiol 2006; 208:487-494.

68. Kaupp UB, Kashikar ND, Weyand I. Mechanisms of sperm chemotaxis. Annu Rev Physiol 2008; 70:93-117.

SUPPLEMENTARY DATA

Movie A: capacitated sperm.

Movie B: procaine-treated sperm.

Movie C: 4-AP-treated sperm.

Movie D: thimerosal-treated sperm.

Movie E: control sperm.

Movie F: Ca^{2+} dynamics of 4-AP-treated sperm. Images were collected at 4 frames/sec and played at 8 frames/sec.

Movie G: Ca^{2+} dynamics of control sperm. Images were collected at 4 frames/sec and played at 8 frames/sec.

Movie H: Ca^{2+} dynamics of thimerosal-treated sperm. Images were collected at 4 frames/sec and played at 8 frames/sec.

Movie I: Ca^{2+} dynamics of control sperm. Images were collected at 4 frames/sec and played at 8 frames/sec.

Movie J: pH dynamics of 4-AP-treated sperm. Images were collected at 4 frames/sec and played at 8 frames/sec.

Movie K: pH dynamics of thimerosal-treated sperm. Images were collected at 4

frames/sec and played at 8 frames/sec.

Movie L: pH dynamics of control sperm. Images were collected at 4 frames/sec and played at 8 frames/sec.

CHAPTER 3

Unexpected flagellar movement patterns and epithelial binding behavior of mouse sperm in the oviduct

ABSTRACT

In order to understand better how sperm movement is regulated in the oviduct, we mated wild-type female mice with Acr-EGFP males, which produce sperm with fluorescent acrosomes. The fluorescence greatly improved our ability to locate sperm moving within the oviduct. Oviducts were removed shortly before or after ovulation and placed in observation chambers on a warm microscope stage for videorecording. Hyperactivated sperm in the isthmic reservoir detached frequently from the epithelium and then reattached. Unexpectedly, most sperm found in the ampulla remained bound to epithelium throughout the observation period of several minutes. In both regions, most sperm produced deep flagellar bends in the direction opposite to the hook of the sperm head. This was unexpected, because mouse sperm incubated under capacitating conditions in vitro primarily hyperactivate by producing deep flagellar bends in the same direction as the hook of the head. In vitro, sperm that are treated with thimerosal to release Ca^{2+} from internal stores produce deep anti-hook bends; however, physical factors such as viscous oviduct fluid could also have produced deep anti-hook bends in

oviductal sperm. Sperm were observed to detach from epithelium in both the ampulla and isthmus during strong contractions of the wall of the oviduct. These observations indicate that sperm continue to bind to oviductal epithelium after they leave the isthmic reservoir and may be assisted in detaching by muscular contractions.

INTRODUCTION

Sperm must become hyperactivated in order to fertilize. Hyperactivation is a swimming pattern characterized by high-amplitude, asymmetrical flagellar beating, resulting in circular or helical swimming trajectories on glass slides [1]. This is in contrast to the activated motility in the ejaculate, which is characterized by low-amplitude, symmetrical flagellar beating that produces a progressive and linear swimming pattern on glass slides. Hyperactivation is generally considered to be a part of the capacitation process, a network of membrane changes and signaling events that enable sperm to fertilize oocytes; these processes occur in the female reproductive tract (reviewed by [2]).

In rabbits and mice, it has been observed that sperm begin to hyperactivate in the lower oviduct before ovulation [3-5]. They do this as part of the process of releasing themselves from the sperm storage reservoir (reviewed by ([6], see also [4, 5, 7, 8]). Prior to release, sperm are held in the reservoir by binding to the surface of the oviductal epithelium. There is evidence that release is brought about by a combination of shedding of oviductal binding proteins from the head of the sperm and by initiation of hyperactivation (reviewed by [9]).

Besides enabling sperm to move beyond the oviductal storage reservoir, hyperactivation plays other roles in assisting sperm to reach the oocytes. Hyperactivation provides sperm with a greater thrusting force to swim through oviductal mucus and to penetrate the viscoelastic cumulus matrix surrounding the

oocyte [10-12]. In addition, hyperactivation is required by sperm to penetrate the zona pellucida of the oocyte in order to reach and fuse with the oocyte plasma membrane [13-15]. The importance of hyperactivation was confirmed by the production of mice with null mutations for *CatSper* genes. The protein products of these genes form plasma membrane Ca^{2+} channels that are pH-sensitive and voltage-dependent. CATSPER channels are only expressed in male germ cells and are located in the plasma membrane of the principal piece of the sperm flagellum [14, 15]. CATSPER null male mice are infertile, primarily because their sperm are unable to hyperactivate (see reviews [16-18]). These sperm do not move beyond the storage reservoir in the lower oviduct and, in vitro, they cannot penetrate the zona pellucida [8, 14, 15].

We reported that, when mouse sperm hyperactivate during capacitation in vitro, the amplitude of the flagellar bend that forms in the same orientation as the hook of the head is greatly increased in most sperm, while the bend that forms in the opposite direction remains unaffected. We will refer to this as pro-hook beating (Figure 3.1). We established that pro-hook beating is stimulated by an influx of Ca^{2+} through CATSPER channels and is associated with an increase of intracellular pH [19].

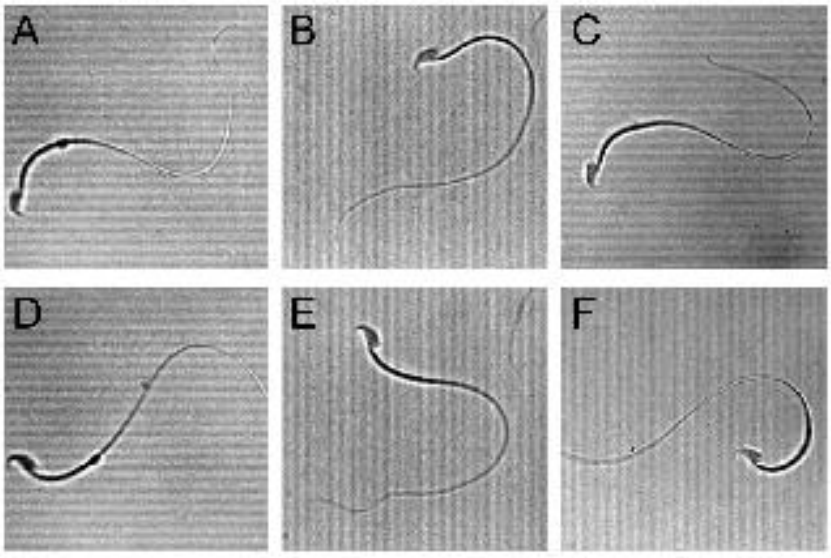

Figure 3.1. Flagellar beating patterns in mouse sperm. The upper row of images (A–C) shows the maximal pro-hook flagellar bends in each flagellar beat pattern, whereas the lower row of images (D–F) shows the maximal anti-hook flagellar bends. A and D: Symmetrical flagellar bends on non-hyperactivated sperm. B and E: Pro-hook flagellar beat pattern. C and F: Anti-hook flagellar beat pattern.

However, we have also demonstrated that we can induce an increase in the bend formed in the opposite direction of the hook by treating sperm with thimerosal to stimulate release of Ca^{2+} from internal stores. We will refer to this as anti-hook beating (Figure 3.1). We also demonstrated that anti-hook beating is dominant over pro-hook beating; that is, when sperm are simultaneously or sequentially subjected to treatments that stimulate pro-hook and anti-hook beating, then the sperm will swim using the anti-hook beating pattern [19]. Switching between pro- and anti-hook beating patterns could modulate the swimming trajectory of sperm in vivo to direct movement of sperm toward oocytes.

In order to understand how sperm movement is regulated in vivo, we undertook this study to examine the movement patterns of sperm leaving the reservoir in the lower isthmus and those few sperm that reach the ampulla of the oviduct. In order to see if the presence of oocytes has an effect on sperm motility, we made our observations in both pre- and post-ovulatory females. We used Acr-EGFP males, which produce sperm with fluorescent acrosomes [20]. This greatly improved our ability to locate sperm moving within the oviduct, especially when the oviduct was left in its natural coiled configuration.

MATERIALS AND METHODS

Media and Chemicals

All routine chemicals and compounds were purchased from Sigma-Aldrich Co. with exceptions noted below.

A capacitation medium for mouse sperm (Suarez and Osman, 1987) was used for incubating oviducts. The medium consisted of 110 mM NaCl, 2.68 mM KCl, 0.36 mM NaH_2PO_4, 25 mM $NaHCO_3$, 25 mM HEPES (EMD Chemicals, Gibbstown, NJ), 5.56 mM glucose, 1.0 mM pyruvic acid, 0.006% penicillin G (Na), 2.4 mM $CaCl_2$, 0.49 mM $MgCl_2$ and 5 mg/ml BSA (EMD Chemicals). The osmolarity range was 290-310 mOsm/kg and the pH was adjusted to 7.6. The medium was sterilized by

filtration through a 0.22 μm membrane filter (Corning Inc., Corning, NY). Before use, it was equilibrated at 37°C with 5% CO_2 in humidified air.

Animals

A hybrid cross (C57BL/6J x BALB/cByJ) of wild-type F1 females aged 8 to 16 weeks was obtained from Dr. John Schimenti (Department of Biomedical Sciences, Cornell University). Male mice aged 10-16 weeks were obtained from Dr. Harvey Florman (Department of Cell Biology, University of Massachusetts Medical School). These mice were hemizygous for the Acr-EGFP transgene. All procedures were approved by the Institutional Animal Care and Use Committee at Cornell.

Superovulation and Mating

To establish the time of ovulation, female mice were injected with 10 IU pregnant mare serum gonadotropin (PMSG) (VWR, Radnor, PA) followed by 10 IU human chorionic gonadotropin (hCG) (VWR) 48 h later [21].

Matings were timed to occur 4-6 h after hCG injection for pre-ovulatory studies and 11-13 h for post-ovulatory studies. To mate mice, a single hormonally stimulated female was introduced to the cage of a singly housed male. Time of ejaculation was recorded when the male suddenly and briefly became very still while grasping the female. Females were left undisturbed with the male for three hours after

mating in order to allow time for sperm transport. At that time, the females were euthanized by CO_2 inhalation to obtain oviducts.

Data were collected from experiments in which 3 males were mated with a total of 6 pre- and 6 post-ovulatory females.

Oviduct preparation

Immediately after euthanization of female mice, oviducts were accessed by abdominal incision. They were removed by grasping the uterine horn at the cranial tip with a pair of fine forceps, then cutting through the uterine horn and the suspensory ligaments. The two oviducts were submerged in separate 35-mm Petri dishes in the medium described above. One oviduct was chosen at random for immediate further dissection and videotaping; the other oviduct was incubated at 37 ℃ under 5% CO_2 in humidified air until videotaping had been completed on the first oviduct, about 20-35 min later.

Further dissection was conducted under a dissecting microscope. The ovary was removed by cutting through the ovarian bursa. Then, the mesosalpinx of each oviduct was trimmed with fine spring surgical scissors to ensure that oviducts were kept as close as possible to the original coiled condition, but not covered by too much mesosalpinx, which occludes visibility of the oviduct lumen. Oviductal dissection was completed within 4-6 min.

Prior to the dissection, microscope chambers were prepared as previously described [8]. Briefly, a standard 75 mm × 25 mm microscope slide was cut in thirds crosswise. A 50 mm × 24 mm #1 coverslip was used to replace the middle third and was glued to the outer two thirds using Krazy Glue (Elmer's, Columbus, OH, USA). A ring of silicone grease (Dow Corning, Midland, MI, USA) was made on the coverslip using a syringe.

Immediately after dissection of the oviduct, it was placed in a droplet of medium in the center of the grease ring on the coverslip. A 25 mm × 25 mm #1 coverslip was placed over the oviduct and pressed down gently onto the silicone grease to hold the oviduct in place. Because the oviduct was held between two coverslips, the chamber could be flipped on the microscope stage in order to find the best views of the oviductal lumen.

Recording sperm behavior in the oviducts

Sperm were located in the oviducts by briefly using epiflourescence microscopy (<10 sec) to detect the green fluorescence. Fluorescence was detected using 10 and 20X objectives with a 480 ± 40 nm excitation filter, 535 ± 50 nm emission filter, and a 505 nm long-pass dichroic mirror (Chroma Technology Corp., Rockingham, VT) with light from a mercury lamp (Model 910426, Carl Zeiss, Inc. Hawthorne, NY).

As soon as motile sperm were located in a region, the light from the mercury lamp was blocked and the region was viewed using 300X brightfield optics. A CCD 72 video camera (DAGE MTI, Michigan City, IN, USA) was used to record sperm in the lower isthmus (LI) and ampulla (AMP) onto SuperVHS videotape (Maxwell Professional SVHS, Osaka, Japan) in a JVC SR-S365U SuperVHS Video Cassette Recorder (JVC, Long Beach, CA, USA). Sperm found in each microscope field were recorded for 2 min. The total number of sperm found in both ampullae was determined. The temperature of the chamber was maintained at 37 ℃ by a stage warmer throughout each experiment and the sealed chamber prevented evaporation and impeded gas exchange with the air.

In addition to the 12 matings described above, 5 extra matings (2 pre- and 3 post-ovulatory females) were conducted in which prolonged observations of individual sperm in the ampullae were made.

Sperm motility patterns were categorized by reviewing the digitized videos. Sperm were scored as “bound” if they attached without detaching during the observation period of 2 min. If at least one free swimming incident was seen during the observation period, the sperm were scored as “free”. The bending direction of sperm flagella in reference to the hook of sperm head was also scored as dominant pro-hook, dominant anti-hook or symmetrical (Figure 3.1). For some sperm, the bending direction could not be determined, because sperm flagella could not be focused or were bent or stuck. Those sperm were scored as “could not determine”.

RESULTS

In the isthmus, sperm frequently detached and reattached while using the anti-hook beating pattern

Three hours after mating, the lumen of the lower half (first two coils) of the isthmus was so crowded with sperm that it was impossible to count them. In the central channel of the lumen, there were some clusters of immotile sperm that were moved back and forth by fluid flow produced by intermittent contractions of the oviduct wall. Motile sperm surrounded these clusters and filled the pockets created in the wall by transverse mucosal folds.

More hyperactivated sperm were seen in the post-ovulatory oviduct in the lower isthmus than in the pre-ovulatory oviduct. In four out of six pairs of pre-ovulatory oviducts, almost none of the sperm were hyperactivated; whereas, a small fraction of hyperactivated sperm was seen in the oviducts of the other two preovulatory females. In contrast, five out of six postovulatory oviducts contained mostly hyperactivated sperm in the lower isthmus. In the remaining pair of postovulatory oviducts, both hyperactivated and non-hyperactivated sperm were seen; however, there were visibly more hyperactivated sperm than non-hyperactivated.

Some of the hyperactivated sperm detached and reattached frequently, whereas others swam freely in the lumen in apparently random directions. In both cases, the hyperactivated sperm showed deep anti-hook bending characteristic of the anti-hook beat pattern (Figure 3.2, see also the Supplemental Movies A and B). Groups of non-

hyperactivated sperm were seen sticking to the wall of the isthmus at the bases of the folds, beating at a steady and rapid rate with low amplitude, symmetrical flagellar bends (Figure 3.3 and Supplemental Movie C).

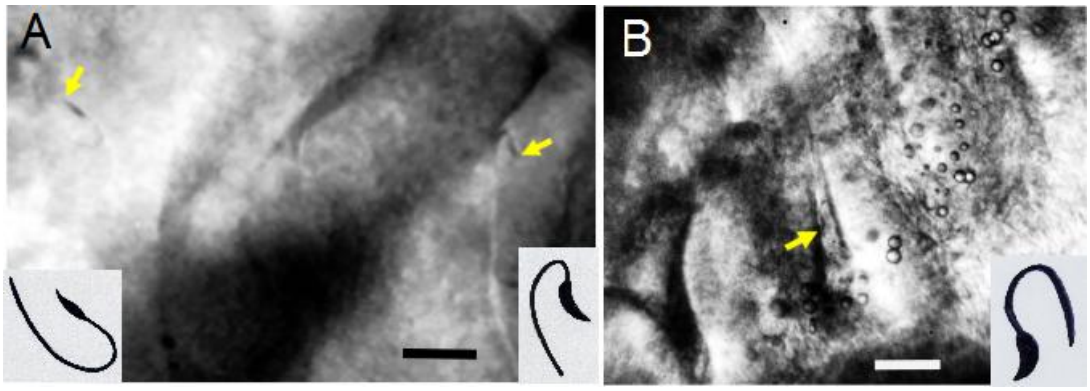

Figure 3.2. **A:** Two free swimming sperm in the isthmus exhibiting deep anti-hook bends of the anti-hook beat pattern. **B:** A sperm exhibiting a deep anti-hook bend at the moment of detaching from epithelium. Yellow arrows: the tip of the hook-shaped head; inserts: tracings of sperm. Images are taken from the Supplemental Movies A and B. Bars indicate 20 μm.

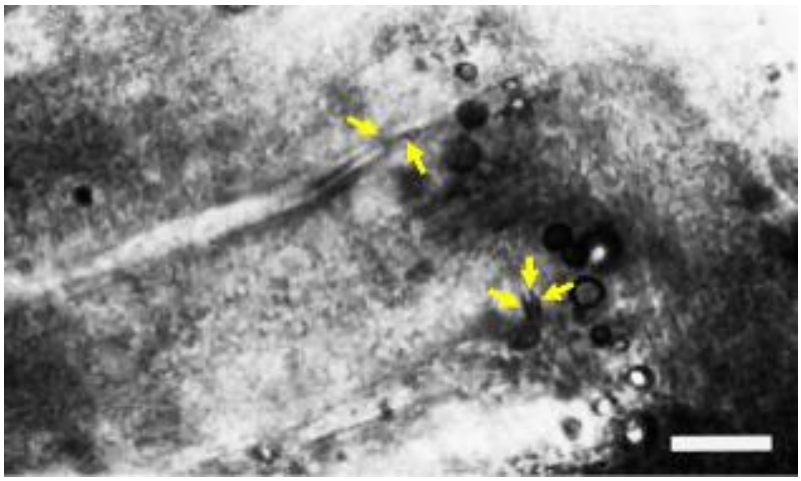

Figure 3.3. Non-hyperactivated sperm in pockets formed by mucosal folds in the

isthmus, taken from the Supplemental Movie C. The yellow arrows indicate the locations of the heads of the sperm that can be seen more clearly in the movie. The bar indicates 20 μm.

In the ampulla, most sperm were bound to the epithelium and used the anti-hook beat pattern

A total of 23 ampullary sperm were found in 6 pre-ovulatory females whereas 88 were found in 6 post-ovulatory females (Table 3.1). Further analysis revealed that 92 ±16.1% and 92% ±4.4% sperm were motile in pre- and post-ovulatory ampullae, respectively. All of the sperm detected in the lumen of the ampulla had green fluorescence in their acrosomes, indicating that they had not undergone the acrosome exocytosis.

Most motile sperm found in both pre- and post-ovulatory ampullae remained bound to the oviductal epithelium during each 2 min videotaping period (Table 3.1). Most of the bound sperm that could be clearly seen exhibited the deep anti-hook bending of the anti-hook beat pattern (Table 3.1, Figure 3.4 and Supplemental Movie D).

Table 3.1. Numbers of sperm showing various flagellar beating patterns in the ampulla.

Exp. No.	Ovulation status	Motile							Immotile	Total
		Bending direction of bound sperm				Bending direction of detaching/reattaching or free swimming sperm				
		Anti	Pro	Symme-trical	Could not deter-mine	Anti	Pro	Could not deter-mine		
1	Pre	2	0	0	1	0	0	0	2	5
2		1	0	0	2	0	0	0	0	3
3		4	0	0	2	1	0	1	1	9
4		0	0	1	1	0	0	0	0	2
5		2	0	0	1	0	0	0	0	3
6		0	0	0	1	0	0	0	0	1
Total		9	0	1	8	1	0	1	3	23
1	Post	9	0	1	2	1	0	0	2	15
2		8	1	0	7	1	0	0	0	17
3		5	1	0	2	1	0	0	1	10
4		6	0	1	2	0	1	1	1	12
5		11	0	2	3	2	0	1	2	21
6		8	0	1	2	1	0	0	1	13
Total		47	2	5	18	6	1	2	7	88

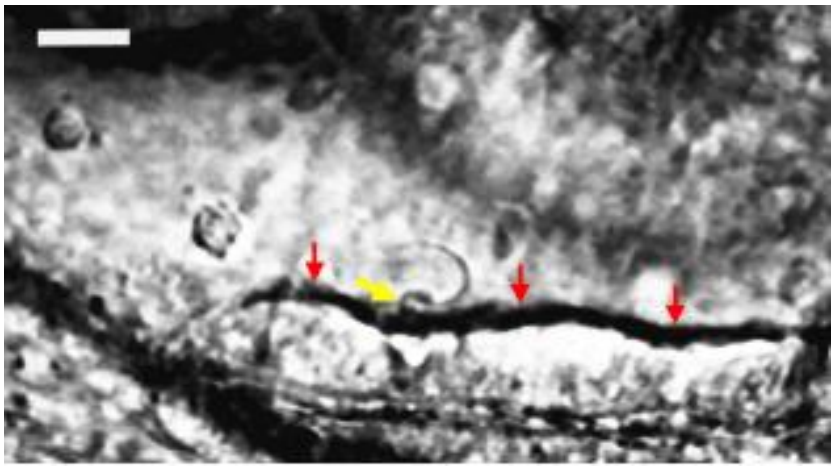

Figure 3.4. An example of a bound sperm showing a deep anti-hook bend in the ampulla. Yellow arrow: tip of hook in sperm head; red arrows: a ridge of ciliated epithelial cells. The image is taken from the Supplemental Movie D. The bar indicates 20 μm.

Smooth muscle contraction in the oviductal wall appeared to assist bound sperm in detaching from epithelium in the ampulla

In order to see whether and how the bound sperm eventually broke free from attachment to the epithelium, prolonged recordings were made of sperm in the ampulla. This type of observation was repeated five times, using two pre- and three post-ovulatory females. All five prolonged observations showed that sperm detached from the epithelium only during strong contractions of the wall of the ampulla (Figure 3.5, see also the Supplemental Movie E). In the post-ovulatory oviducts, cumulus-oocyte-complexes (COCs) were seen to move back and forth in the ampullary lumen with each contraction (Figure 3.6, see also the Supplemental Movie F). Sperm could not be detected in the COCs.

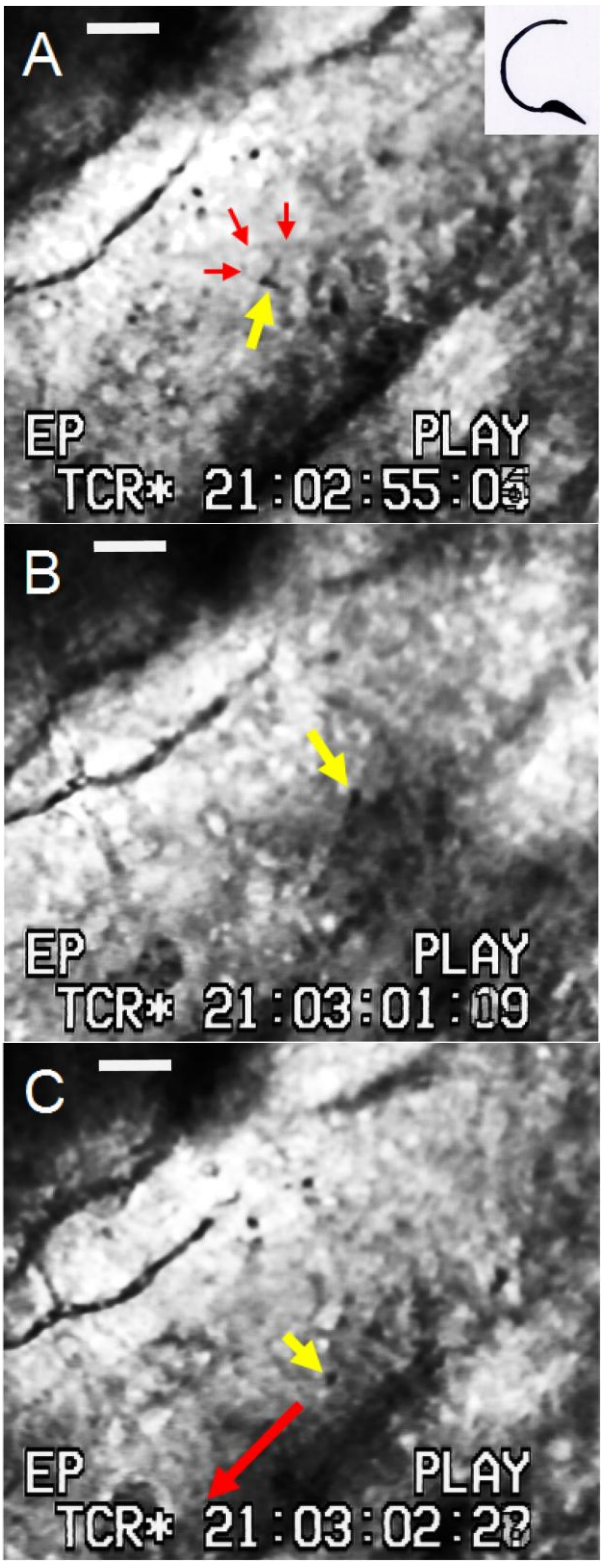

Figure 3.5. An example of sperm detaching from the epithelium in the ampulla

during strong contractions of the oviduct wall, taken from the Supplemental Movie E. The sperm can be seen more clearly in the movie. The sperm head is indicated by yellow arrows. **A:** A sperm bound to the ampulla wall before contraction. Red arrows indicate the sperm flagellum. Insert: tracing of the sperm. **B:** This sperm still bound to the ampulla wall at the beginning of contraction. **C:** The moment that this sperm detached during wall contraction. Red arrow: the direction in which the sperm moved after detachment. Bars indicate 20 μm.

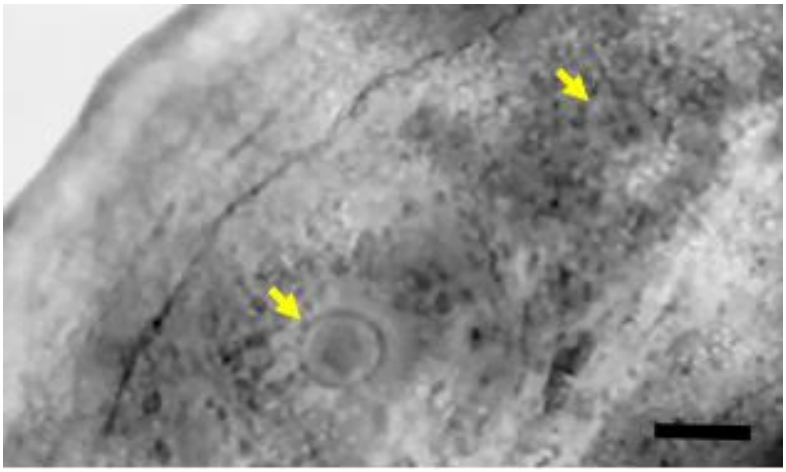

Figure 3.6. COCs in the ampulla. Yellow arrows: oocytes surrounded by the cumulus. The image is taken from the Supplemental Movies F. The bar indicates 100 μm.

DISCUSSION

In this study, we characterized and compared mouse sperm motility patterns in the lower isthmus (site of the sperm reservoir) and the ampulla (site of fertilization) in both pre- and post-ovulatory females. Our observations indicate that sperm movement differs in the two regions: hyperactivated sperm frequently detached and reattached in

the lower isthmus, whereas they remained bound to oviductal epithelium for extended periods in the ampulla. The deep anti-hook beat pattern was the predominant flagellar beating pattern of hyperactivated sperm in both regions. In addition, more ampullary sperm were found in the post-ovulatory females than pre-ovulatory females. This confirmed that sperm transport to fertilization site is facilitated when ovulation occurs, because sperm had been in the female tract for 3 h in both cases.

We found that the flagella of most sperm in the isthmus and ampulla beat in the anti-hook pattern. We had reported previously that isthmic sperm produce deep anti-hook bends immediately before detaching from the oviductal epithelium [8]. In contrast to what we observed in the oviduct, in vitro, most motile sperm incubated in capacitating medium develop pro-hook beat patterns [19]; this pattern could also be seen in figures of sperm capacitated in vitro published previously by us and others [22-24].

The environment of mouse sperm in vivo is quite different from that provided by capacitation media used for in vitro experiments. First, the oviductal fluid of mice and other species contains amino acids, carbohydrates, hormones, growth factors, purinergic agents, glycoproteins and neurotransmitters ([25-28], reviewed by [29]) that are absent in capacitation media. Sperm have been reported to contain various receptors, especially hormone and neurotransmitter receptors (reviewed by [30, 31]) and could therefore respond to these additional components of oviduct fluid. Furthermore, the levels of ions and pH in mouse oviductal fluid are unknown. It is likely that mouse sperm capacitate differently in vivo than in vitro, such that sufficient

Ca^{2+} release is triggered from the intracellular Ca^{2+} stores to cause anti-hook flagellar beating. We previously reported that anti-hook beating was triggered by stimulating release of Ca^{2+} from internal stores and that it was dominant over pro-hook beating stimulated by in vitro capacitation or treatment with procaine or 4-amino pyridine to activate CATSPER channels [19].

Second, sperm encounter a viscous or even viscoelastic fluid in the oviduct; whereas, a low-viscosity medium is used to capacitate sperm in vitro. In all fluid, at the small scale of the size of sperm, viscosity dominates over inertia and strongly affects the pattern of sperm flagellar beating. Although even aqueous media are experienced by sperm as being highly viscous, increases in viscosity due to the presence of large molecules such as those that comprise oviductal mucus greatly increase the resistance to movement felt by sperm (reviewed by [32]). When capacitated mouse sperm with pro-hook bending were placed in medium in which the viscosity or viscoelasticity had been increased by adding methylcellulose or long-chain polyacrylamide, respectively, sperm swam in a relatively straight trajectory with small, sharp anti-hook bends [22]. In vivo, therefore, the viscosity and elasticity of oviduct fluid could promote anti-hook bending. The viscosity in the oviduct is greater than that in capacitation medium, due to the presence of mucous secretions in the uterotubal junction and isthmus in various species such as rabbits, humans, pigs and dairy cattle ([33-35], reviewed by [6]).

Third, sperm binding to epithelium could affect sperm flagellar beating. The physical aspect of binding alone, however, would not be the main reason, because we

have not seen anti-hook beating in sperm capacitated in vitro and stuck by their heads to glass slides (data not shown), nor have we seen it in published figures of sperm with tethered heads [36, 37]. Instead, oviductal epithelium might stimulate sperm directly through receptor/ligand interactions or through local secretions. Both ampullary and isthmic epithelium contain secretory and ciliated cells; in mice, the secretory cells are dominant in the isthmus [38].

The use of mouse epididymal sperm rather than ejaculated sperm for in vitro experiments should also be taken into account when considering why the behavior of sperm might be different in vitro than in vivo. For example, one obvious morphological difference is that many epididymal sperm have a cytoplasmic droplet at the annulus, whereas the sperm we examined in vivo did not have this structure. Shedding of the cytoplasmic droplet is associated with the shear force brought by ejaculation and is proposed to be necessary for fertility ([39], reviewed by [40, 41]). In addition, during ejaculation, epididymal sperm mix with fluids from the seminal vesicles, the prostate and the bulbourethral glands, which could affect flagellar beat patterns.

Hyperactivated sperm in the lower isthmus were seen to detach and reattach frequently (Figure 3.2, see also the Supplemental Movies A and B). Non-hyperactivated sperm attached to the epithelium in groups and beat with low amplitude, symmetrical bends (Figure 3.3, see also Supplemental Movie C). We also noticed that sperm in the central lumen of isthmus were more subject to the fluid flow

caused by contraction than sperm in the pockets formed by mucosal folds, as reported in previous publications [7, 8].

Although hyperactivated sperm in the peri-ovulatory isthmus were seen to detach and reattach, sperm that were bound to the epithelium in the ampulla rarely detached. Only a few were seen swimming freely before reattaching to the epithelium (Table 3.1). This may be due to the greater numbers of ciliated cells in the ampulla. For some sperm videotaped in the ampulla, we could clearly see them bind to cilia (Figure 3.4, see also the Supplemental Movie D). In mice, both the ampullary and isthmic epithelium contain secretory and ciliated cells; however, ciliated cells predominate in the ampulla whereas secretory cells predominate in the isthmus [38]. The observation of prolonged binding of sperm in the ampulla differs from a previous report, where more free swimming sperm were seen in the ampulla [7]. This discrepancy could be due to the method of handling the oviducts. In our previous study, the mesosalpinx was completely removed in order to uncoil the entire oviduct; whereas, in this study, we left it in the original coiled condition to the extent possible. Excess manipulation of the oviduct could detach sperm from the epithelium or move detached sperm from the isthmus to the ampulla.

Sperm in the ampulla were only seen to detach from epithelium after a muscle contraction, although not all contractions brought about sperm detachment. Detachment could be caused by the physical force of the luminal fluid pushed by the contraction, or to chemical signaling molecules brought by fluid flow to trigger the release of sperm, or both. How sperm sense and respond to physical force is largely

unknown. In many cell types, members of the TRP channel family detect a variety of physical and chemical stimuli and introduce Ca^{2+} influx to control cell behaviors. Various TRP channels have been identified in mammalian sperm but their roles, especially in sensing physical stimuli, are not completely understood ([42], see also the review by [43]).

Many studies suggest that smooth muscle contraction of the female reproductive tract plays a role in sperm as well as oocyte transport. It is thought that sperm are transported through the uterus mainly by smooth muscle contraction (reviewed by [6]). In the oviduct, contraction is regulated by the endocrine and autonomic nervous systems, but is also somewhat autonomous ([44, 45], reviewed by [46]). Hormones could affect the autonomous contraction as well by stimulating the oviductal pacemaker cells [47-49]. Oviductal contraction has been proposed to direct sperm toward the ampulla in pigs and hamsters during the peri-ovulatory period [50, 51]. Interestingly, Dixon *et al.* reported that the COCs were transported through the ampulla in a back-and-forth swinging manner, with a net contractile movement directed toward the uterus. Blocking propagating contraction eliminated the movement of COCs, whereas the ciliary beating was unaffected [45]. It is difficult to understand how sperm might be transported toward the ovary in the ampulla, when the net movement of the contractions is toward the uterus.

All sperm found in the ampulla had fluorescent acrosomes. It is possible, however, that we missed acrosome-reacted sperm. Recent work suggests that acrosome exocytosis of mouse sperm occurs mainly in the cumulus, while some

occurs on the zona pellucida ([52], reviewed by [53]).

We found that we were able to detect more sperm in the ampulla when using fluorescently labeled acrosomes than when we used wild-type sperm, particularly when the oviduct was left in the natural coiled position. The improved detection of sperm led to two new observations. The first was that the flagella of most sperm in the oviduct beat in the anti-hook pattern, indicating that the internal Ca^{2+} store is likely to play a role in moving sperm in the oviduct. The second is that the few sperm that reached the oviductal ampulla spent most of their time tightly bound to the epithelium and may only have been dislodged by contractions of the wall of the oviduct. This may be a mechanism for holding sperm in the lower-to-mid ampulla until the COCs arrive.

REFERENCES

1. Yanagimachi R. The movement of golden hamster spermatozoa before and after capacitation. J Reprod Fertil 1970; 23:193-196.

2. Visconti PE. Understanding the molecular basis of sperm capacitation through kinase design. Proc Natl Acad Sci U S A 2009; 106:667-668.

3. Overstreet JW, Cooper GW. Effect of ovulation and sperm motility on the migration of rabbit spermatozoa to the site of fertilization. J Reprod Fertil 1979; 55:53-59.

4. Suarez SS, Osman RA. Initiation of hyperactivated flagellar bending in mouse sperm within the female reproductive tract. Biol Reprod 1987; 36:1191-1198.

5. Pacey AA, Davies N, Warren MA, Barratt CL, Cooke ID. Hyperactivation may assist human spermatozoa to detach from intimate association with the endosalpinx. Hum Reprod 1995; 10:2603-2609.

6. Suarez SS, Pacey AA. Sperm transport in the female reproductive tract. Hum Reprod Update 2006; 12:23-37.

7. DeMott RP, Suarez SS. Hyperactivated sperm progress in the mouse oviduct. Biol Reprod 1992; 46:779-785.

8. Ho K, Wolff CA, Suarez SS. CatSper-null mutant spermatozoa are unable to ascend beyond the oviductal reservoir. Reprod Fertil Dev 2009; 21:345-350.

9. Suarez SS. Regulation of sperm storage and movement in the mammalian oviduct. Int J Dev Biol 2008; 52:455-462.

10. Suarez SS, Katz DF, Owen DH, Andrew JB, Powell RL. Evidence for the function of hyperactivated motility in sperm. Biol Reprod 1991; 44:375-381.

11. Suarez SS, Dai XB, DeMott RP, Redfern K, Mirando MA. Movement characteristics of boar sperm obtained from the oviduct or hyperactivated in vitro. J Androl 1992; 13:75-80.

12. Quill TA, Sugden SA, Rossi KL, Doolittle LK, Hammer RE, Garbers DL. Hyperactivated sperm motility driven by CatSper2 is required for fertilization. Proc Natl Acad Sci U S A 2003; 100:14869-14874.

13. Stauss CR, Votta TJ, Suarez SS. Sperm motility hyperactivation facilitates penetration of the hamster zona pellucida. Biol Reprod 1995; 53:1280-1285.

14. Ren D, Navarro B, Perez G, Jackson AC, Hsu S, Shi Q, Tilly JL, Clapham DE. A sperm ion channel required for sperm motility and male fertility. Nature 2001; 413:603-609.

15. Quill TA, Ren D, Clapham DE, Garbers DL. A voltage-gated ion channel expressed specifically in spermatozoa. Proc Natl Acad Sci U S A 2001; 98:12527-12531.

16. Navarro B, Kirichok Y, Chung JJ, Clapham DE. Ion channels that control fertility in mammalian spermatozoa. Int J Dev Biol 2008; 52:607-613.

17. Publicover SJ, Giojalas LC, Teves ME, de Oliveira GS, Garcia AA, Barratt CL, Harper CV. Ca2+ signalling in the control of motility and guidance in mammalian sperm. Front Biosci 2008; 13:5623-5637.

18. Suarez SS. Control of hyperactivation in sperm. Hum Reprod Update 2008; 14:647-657.

19. Chang H, Suarez SS. Two distinct Ca2+ signaling pathways modulate sperm

flagellar beating patterns in mice. Biol Reprod 2011; 85:296-305.

20. Nakanishi T, Ikawa M, Yamada S, Parvinen M, Baba T, Nishimune Y, Okabe M. Real-time observation of acrosomal dispersal from mouse sperm using GFP as a marker protein. FEBS Lett 1999; 449:277-283.

21. Laboratory J. Superovulation technique. Jax Notes 1988; 1988;434.

22. Suarez SS, Dai X. Hyperactivation enhances mouse sperm capacity for penetrating viscoelastic media. Biol Reprod 1992; 46:686-691.

23. Visconti PE, Bailey JL, Moore GD, Pan D, Olds-Clarke P, Kopf GS. Capacitation of mouse spermatozoa. I. Correlation between the capacitation state and protein tyrosine phosphorylation. Development 1995; 121:1129-1137.

24. Marquez B, Ignotz G, Suarez SS. Contributions of extracellular and intracellular Ca2+ to regulation of sperm motility: Release of intracellular stores can hyperactivate CatSper1 and CatSper2 null sperm. Dev Biol 2007; 303:214-221.

25. Revelli A, Delle Piane L, Casano S, Molinari E, Massobrio M, Rinaudo P. Follicular fluid content and oocyte quality: from single biochemical markers to metabolomics. Reprod Biol Endocrinol 2009; 7:40.

26. Burrello N, Vicari E, D'Amico L, Satta A, D'Agata R, Calogero AE. Human follicular fluid stimulates the sperm acrosome reaction by interacting with the gamma-aminobutyric acid receptors. Fertil Steril 2004; 82 Suppl 3:1086-1090.

27. Leese HJ, Tay JI, Reischl J, Downing SJ. Formation of Fallopian tubal fluid: role of a neglected epithelium. Reproduction 2001; 121:339-346.

28. Harris SE, Gopichandran N, Picton HM, Leese HJ, Orsi NM. Nutrient concentrations in murine follicular fluid and the female reproductive tract. Theriogenology 2005; 64:992-1006.

29. Leese HJ, Hugentobler SA, Gray SM, Morris DG, Sturmey RG, Whitear SL, Sreenan JM. Female reproductive tract fluids: composition, mechanism of formation and potential role in the developmental origins of health and disease. Reprod Fertil Dev 2008; 20:1-8.

30. Naz RK, Sellamuthu R. Receptors in spermatozoa: are they real? J Androl 2006; 27:627-636.

31. Meizel S. The sperm, a neuron with a tail: 'neuronal' receptors in mammalian

sperm. Biol Rev Camb Philos Soc 2004; 79:713-732.

32. Kirkman-Brown JC, Smith DJ. Sperm motility: is viscosity fundamental to progress? Mol Hum Reprod 2011; 17:539-544.

33. Jansen RP. Fallopian tube isthmic mucus and ovum transport. Science 1978; 201:349-351.

34. Jansen RP, Bajpai VK. Oviduct acid mucus glycoproteins in the estrous rabbit: ultrastructure and histochemistry. Biol Reprod 1982; 26:155-168.

35. Suarez SS, Brockman K, Lefebvre R. Distribution of mucus and sperm in bovine oviducts after artificial insemination: the physical environment of the oviductal sperm reservoir. Biol Reprod 1997; 56:447-453.

36. Morgan DJ, Weisenhaus M, Shum S, Su T, Zheng R, Zhang C, Shokat KM, Hille B, Babcock DF, McKnight GS. Tissue-specific PKA inhibition using a chemical genetic approach and its application to studies on sperm capacitation. Proc Natl Acad Sci U S A 2008; 105:20740-20745.

37. Carlson AE, Burnett LA, del Camino D, Quill TA, Hille B, Chong JA, Moran MM, Babcock DF. Pharmacological targeting of native CatSper channels reveals a required role in maintenance of sperm hyperactivation. PLoS One 2009; 4:e6844.

38. Yamanouchi H, Umezu T, Tomooka Y. Reconstruction of oviduct and demonstration of epithelial fate determination in mice. Biol Reprod 2010; 82:528-533.

39. Yeung CH, Wagenfeld A, Nieschlag E, Cooper TG. The cause of infertility of male c-ros tyrosine kinase receptor knockout mice. Biol Reprod 2000; 63:612-618.

40. Cooper TG. Cytoplasmic droplets: the good, the bad or just confusing? Hum Reprod 2005; 20:9-11.

41. Cooper TG. The epididymis, cytoplasmic droplets and male fertility. Asian J Androl 2011; 13:130-138.

42. De Blas GA, Darszon A, Ocampo AY, Serrano CJ, Castellano LE, Hernandez-Gonzalez EO, Chirinos M, Larrea F, Beltran C, Trevino CL. TRPM8, a versatile channel in human sperm. PLoS One 2009; 4:e6095.

43. Clapham DE. SnapShot: mammalian TRP channels. Cell 2007; 129:220.

44. Battalia DE, Yanagimachi R. The change in oestrogen and progesterone levels triggers adovarian propulsive movement of the hamster oviduct. J Reprod Fertil 1980; 59:243-247.

45. Dixon RE, Hwang SJ, Hennig GW, Ramsey KH, Schripsema JH, Sanders KM, Ward SM. Chlamydia infection causes loss of pacemaker cells and inhibits oocyte transport in the mouse oviduct. Biol Reprod 2009; 80:665-673.

46. Hunter RH. Sperm release from oviduct epithelial binding is controlled hormonally by peri-ovulatory graafian follicles. Mol Reprod Dev 2008; 75:167-174.

47. Cretoiu D, Ciontea SM, Popescu LM, Ceafalan L, Ardeleanu C. Interstitial Cajal-like cells (ICLC) as steroid hormone sensors in human myometrium: immunocytochemical approach. J Cell Mol Med 2006; 10:789-795.

48. Cretoiu SM, Cretoiu D, Suciu L, Popescu LM. Interstitial Cajal-like cells of human Fallopian tube express estrogen and progesterone receptors. J Mol Histol 2009; 40:387-394.

49. Popescu LM, Ciontea SM, Cretoiu D. Interstitial Cajal-like cells in human uterus and fallopian tube. Ann N Y Acad Sci 2007; 1101:139-165.

50. Blandau RJ, Gaddum-Rosse P. Mechanism of sperm transport in pig oviducts. Fertil Steril 1974; 25:61-67.

51. Battalia DE, Yanagimachi R. Enhanced and co-ordinated movement of the hamster oviduct during the periovulatory period. J Reprod Fertil 1979; 56:515-520.

52. Jin M, Fujiwara E, Kakiuchi Y, Okabe M, Satouh Y, Baba SA, Chiba K, Hirohashi N. Most fertilizing mouse spermatozoa begin their acrosome reaction before contact with the zona pellucida during in vitro fertilization. Proc Natl Acad Sci U S A 2011; 108:4892-4896.

53. Bedford JM. Site of the mammalian sperm physiological acrosome reaction. Proc Natl Acad Sci U S A 2011; 108:4703-4704.

SUPPLEMENTARY DATA

Movie A: Hyperactivated sperm in the isthmus showing the anti-hook beat pattern. Movie plays in real time.

Movie B: Hyperactivated sperm in the isthmus showing the anti-hook beat pattern. Movie plays in real time.

Movie C: Non- hyperactivated sperm in the isthmus. Movie plays in real time.

Movie D: A bound sperm in the ampulla showing the anti-hook beat pattern. Movie plays in real time.

Movie E: A sperm detaching from the epithelium during contraction of the ampulla. Movie plays in real time.

Movie F: The movement of COCs during contraction of the ampulla. Movie plays in real time.

CHAPTER 4

Conclusion

This dissertation was inspired by the working hypothesis that mammalian sperm motility is modulated to guide the ascent of sperm up the oviduct and toward the oocytes. As a graduate student, I came to focus on two projects to interrogate this hypothesis: 1) to distinguish the effects of Ca^{2+} influx through CATSPER channels from those of Ca^{2+} release from redundant nuclear envelope (RNE) stores; 2) To determine the flagellar movement patterns of sperm in the oviduct.

We found that when mouse sperm hyperactivate during capacitation in vitro, the amplitude of the flagellar bend that forms in the same orientation as the hook of the head is greatly increased, while the bend that forms in the opposite direction remains unaffected. We defined this as pro-hook beating. We established that pro-hook beating is stimulated by an influx of Ca^{2+} through CATSPER channels and is associated with an increase of intracellular pH. However, we have demonstrated that we can induce an increase of flagellar bend amplitude in the opposite direction by treating sperm with thimerosal to stimulate release of Ca^{2+} from internal stores. This is defined as anti-hook beating. We also demonstrated that anti-hook beating is dominant over pro-hook beating; that is, when sperm are simultaneously or sequentially subjected to treatments that stimulate pro-hook and anti-hook beating, then the sperm will swim using the anti-hook beating pattern. Different protein phosphorylation patterns were detected in extracts of sperm that produced these two different flagellar

beat patterns, indicating the involvement of different signaling pathways.

In order to understand how sperm movement is regulated in vivo, we examined the movement patterns of sperm leaving the reservoir in the lower isthmus of the oviduct and those of the few sperm that reach the ampulla of the oviduct during the periovulatory period. In both regions, most sperm produced deep flagellar bends in the anti-hook direction. The reason why the flagellar beating pattern of sperm undergoing capacitation might be different in vitro than in vivo could be due to various factors, including the additional components in the oviduct fluid that are not included in capacitation medium, the viscosity or viscoelasticity of oviductal fluid, sperm binding to the oviductal epithelium, and the changes in sperm brought by ejaculation and exposure to secretions of the male accessory sex glands (please see the Discussion of Chapter 3). If any of the factors stimulates Ca^{2+} release from the intracellular store, this would mask pro-hook bending caused solely by Ca^{2+} influx via CATSPER channels, because stimulation of anti-hook beating was observed to be dominant over stimulation of pro-hook beating.

In addition, we found that hyperactivated sperm in the isthmic reservoir detached frequently from the epithelium and then reattached. In contrast, the few sperm that reached the oviductal ampulla spent most of their time tightly bound to the epithelium and may only have been dislodged by contractions of the wall of the oviduct. At the same time, the cumulus-oocyte-complexes (COCs) were seen to move in a back-and-forth manner in the oviduct. This suggests a possible mechanism for fertilization; that is, sperm are held in the oviductal ampulla by attaching to the wall

and are freed by being swept off of the surface by the movement of the cumulus back and forth during contractions.

In summary, these data and observations contribute to the understanding of how sperm reach oocytes. This process at least requires changes in sperm and interaction between sperm and the oviduct, which also influence and are influenced by ovulation and the presence of COCs.

As it often the case with scientific research, more questions than answers are produced. There are still many questions that have not been answered and would be my potential future focus. For instance, there are publications about contraction moving sperm up to ampulla in pigs and hamsters [1, 2], as opposed to moving the COCs down in the mouse [3]. If the contractions are gradually moving the COC down the mouse ampulla, how can the sperm move up during a contraction? At what point do the sperm begin sticking so tightly to the epithelium such that only contractions can free them? To answer these questions, detailed in vivo observations are required. The direction of contraction and sperm swimming patterns in the oviduct in reference to the direction of contraction would be recorded and analyzed. Oviductal contraction would be blocked to see if sperm could arrive at ampulla. Also, the contraction pattern before and during ovulation would be quantified and compared.

When mammalian sperm reach the vicinity of the oocytes, they may be chemotactically attracted to the oocytes. Progesterone, a steroid hormone secreted from cumulus cells around the oocyte, could form a gradient around COCs and direct

sperm toward the oocyte mass. However, progesterone is reported to play multiple roles, including inducing hyperactivation and acrosome reactions (reviewed by [4]). Recently, both Struncker *et al.* and Lishko *et al.* report that progesterone substantially enhanced current of CATSPER channels on human sperm, whereas such current was not found in epididymal mouse sperm upon progesterone stimulation [5, 6]. To further explore the possibility of progesterone as a chemoattractant, a modified microfluidic chamber [7] could be used to generate a gradient of progesterone or COC extracts to study mouse sperm chemotaxis. We have already tested such a device by testing the responses of sperm of the sea urchin *Arbacia punctulata* to the chemoattractant resact, which is a well-established phenomenon. An immediate chemotactic response was observed when an exponential gradient of resact was generated; however, since the size, swimming speed and swimming trajectory of mouse sperm are very different from sea urchin sperm, this device may require modifications to accommodate the larger size and faster swimming speeds of mouse sperm.

Closely mimicking the in vivo conditions under which chemotaxis would occur is crucial for conducting in vitro experiments, but it is challenging. For example, female oviduct fluid is viscous or even viscoelastic (reviewed by [8]). Viscosity has a dramatic role in affecting sperm movement as well as delaying the spread of a chemical gradient by decreasing the diffusion rate of molecules through the fluid (reviewed by [9]). In addition to the delayed spread of a chemoattractant gradient in vivo, an already-formed gradient could be interrupted by muscle contraction and ciliary beating in the ampulla. Smooth muscle contraction in the oviductal wall exists

all along the oviduct ([3, 10], reviewed by [8, 11], please see the Discussion of Chapter 3). Contraction could interrupt a linear chemoattractant gradient periodically. In addition, the mouse ampulla is dominated by ciliary cells [12]; the "stirring" caused by cilia beating in the ampulla could interfere with the gradient as well. When designing in vitro experiments, those factors should be considered and measured.

In summary, my work as a graduate student provides evidence for specific mechanisms of sperm transport in the oviduct in terms of the cell biology of the sperm and the interactions of sperm with the oviductal epithelium. These data contribute to the understanding of how mammalian sperm reach the oocyte. It is my hope that this information will stimulate the emergence of new ideas for diagnosing and treating infertility, as well as for developing new contraceptives.

REFERENCES

1. Blandau RJ, Gaddum-Rosse P. Mechanism of sperm transport in pig oviducts. Fertil Steril 1974; 25: 61-67.

2. Battalia DE, Yanagimachi R. Enhanced and co-ordinated movement of the hamster oviduct during the periovulatory period. J Reprod Fertil 1979; 56: 515-520.

3. Dixon RE, Hwang SJ, Hennig GW, Ramsey KH, Schripsema JH, Sanders KM, Ward SM. Chlamydia infection causes loss of pacemaker cells and inhibits oocyte transport in the mouse oviduct. Biol Reprod 2009; 80: 665-673.

4. Chang H, Suarez SS. Rethinking the relationship between hyperactivation and chemotaxis in mammalian sperm. Biol Reprod 2010; 83:507-513.

5. Strunker T, Goodwin N, Brenker C, Kashikar ND, Weyand I, Seifert R, Kaupp UB. The CatSper channel mediates progesterone-induced Ca2+ influx in human sperm. Nature 2011; 471: 382-386.

6. Lishko PV, Botchkina IL, Kirichok Y. Progesterone activates the principal Ca2+ channel of human sperm. Nature 2011; 471: 387-391.

7. Haessler U, Kalinin Y, Swartz MA, Wu M. An agarose-based microfluidic platform with a gradient buffer for 3D chemotaxis studies. Biomed Microdevices 2009; 11: 827-835.

8. Suarez SS, Pacey AA. Sperm transport in the female reproductive tract. Hum Reprod Update 2006; 12: 23-37.

9. Kirkman-Brown JC, Smith DJ. Sperm motility: is viscosity fundamental to progress? Mol Hum Reprod 2011; 17: 539-544.

10. Muglia U, Motta PM. A new morpho-functional classification of the Fallopian tube based on its three-dimensional myoarchitecture. Histol Histopathol 2001; 16: 227-237.

11. Vizza E, Muglia U, Macchiarelli G, Baschieri L, Pasetto N, Motta PM. Three-dimensional architecture of the human myosalpinx isthmus. Scanning electron microscopy after NaOH digestion and ultrasonic microdissection. Cell Tissue Res 1991; 266: 219-221.

12. Yamanouchi H, Umezu T, Tomooka Y. Reconstruction of oviduct and demonstration of epithelial fate determination in mice. Biol Reprod 2010; 82: 528-533.

13. Spehr M, Gisselmann G, Poplawski A, Riffell JA, Wetzel CH, Zimmer RK, Hatt H. Identification of a testicular odorant receptor mediating human sperm chemotaxis. Science 2003; 299: 2054-2058.

14. Fukuda N, Yomogida K, Okabe M, Touhara K. Functional characterization of a mouse testicular olfactory receptor and its role in chemosensing and in regulation of sperm motility. J Cell Sci 2004; 117: 5835-5845.